JOC The Journal of Organic Chemistry
Cite This: J. Org. Chem. XXXX, XXX, XXX−XXX
Article
pubs.acs.org/joc

Counteracting in Vitro Toxicity of the Ionophoric Mycotoxin Beauvericin—Synthetic Receptors to the Rescue

Vincent Ornelis,[†] Andreja Rajkovic,[‡] Marlies Decleer,[‡,∥] Benedikt Sas,[§] Sarah De Saeger,[∥] and Annemieke Madder*[,†]

[†]Organic and Biomimetic Chemistry Research Group, Department of Organic and Macromolecular Chemistry, Ghent University, Krijgslaan 281, 9000 Ghent, Belgium

[‡]Department of Food Safety and Food Quality, Laboratory of Food Microbiology and Food Preservation and [§]Department of Food Safety and Food Quality, Food2Know, Ghent University, Coupure Links 653, 9000 Ghent, Belgium

[∥]Department of Bioanalysis, Laboratory of Food Analysis, Ghent University, Ottergemsesteenweg 460, 9000 Ghent, Belgium

Supporting Information

ABSTRACT: Beauvericin (BEA) and enniatins are toxic ionophoric cyclodepsipeptides that mainly occur in grains. As such, their presence in food commodities poses a concern for public health. To date, despite recent European Food Safety Authority emphasis on the need for more data to evaluate long-term toxicity effects, no suitable affinity reagents are available to detect the presence of BEA and derivatives in food samples. We here report on the synthesis of a small library of artificial receptors with varying cavity sizes and different hydrophobic building blocks. Immobilization of one of the receptors on solid support resulted in a strong retention of beauvericin, thus revealing promising properties as solid-phase extraction material for sample pretreatment. Furthermore, treatment of HepG2 cells with the most promising receptor markedly reduced beauvericin-induced cytotoxicity, hinting toward the possibility of using synthetic receptors as antidotes against ionophoric toxins.

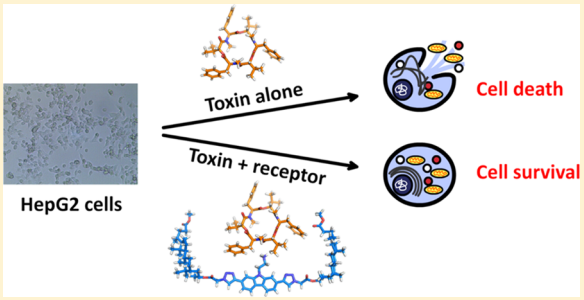

INTRODUCTION

When it comes to food-borne illnesses, most attention goes to the causative microorganisms[1] such as the well-known *Salmonella* spp., *Listeria monocytogenes*, *Staphylococcus aureus*, Shiga toxin-producing *Escherichia coli*, or the less familiar norovirus.[2] Yet, an equally important and often forgotten cause of food poisoning is related to the ingestion of toxins and not to the microorganisms themselves.

Beauvericin (BEA) is a mycotoxin produced by fungi of the *Fusarium* genus, which infect grains such as wheat, barley, and corn.[3] These fungi also produce another kind of cyclodepsipeptide, namely, enniatins (ENN),[4] which only differ slightly in structure from beauvericin (Figure 1) and show comparable toxicity profiles. Quantification of BEA and ENN content in 228 Norwegian grain samples collected at the grain delivery site revealed a high abundance of these toxins (32% of samples contained BEA, 25% ENN A, 67% ENN A_1, 100% ENN B, and 94% ENN B_1). Concentrations up to 7.4 mg/kg were detected for the sum of the toxins.[5] Moreover, infected grain kernels have been shown to contain as much as 520 mg/kg beauvericin.[6] The observation that ENN B is frequently the most abundant enniatin subtype found in grain samples has also been confirmed by others.[7] Due to their thermal stability, these toxins survive most food-processing techniques, which explains their presence in food commodities.

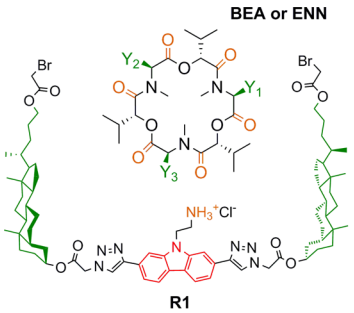

	Y_1	Y_2	Y_3
BEA	Bn	Bn	Bn
ENN A	sBu	sBu	sBu
ENN A1	sBu	sBu	iPr
ENN B	iPr	iPr	iPr
ENN B1	iPr	iPr	sBu

Figure 1. Chemical structure of receptor **R1** with color-coded indication of the possible interactions with BEA or the most common ENN subtypes.

The primary toxic action of BEA and ENN is related to their ability to form ion channels and transport NH_4^+ or K^+ ions across the cell membrane, resulting in disturbance of the ion homeostasis and eventually cell death.[8] As reported by Tonshin and co-workers, addition of 3.8 μM BEA causes membrane depolarization of human neural Paju cells.[9]

Received: June 21, 2019

DOI: 10.1021/acs.joc.9b01665
J. Org. Chem. XXXX, XXX, XXX−XXX

Concentrations in the range of 10 μM are cytotoxic,[10] and due to its lipophilic nature, beauvericin has been shown to accumulate in the liver and adipose tissue.[11] Moreover, passage through the blood−brain barrier has also been shown.[12]

This combination of toxic properties with the occurrence in food commodities poses a considerable risk to human health. In contrast to a variety of commercial immunoaffinity cartridges being available for sample preparation in food analysis for other mycotoxins (such as aflatoxins, deoxynivalenol, zearalenone, or fumonisins) and given the unavailability of antibodies or other suitable retention molecules, there is currently a complete lack of suitable tools for detection of BEA and derivatives in food. Furthermore, no antidote is available against BEA, ENN, or related ionophores, which is also attributed to the difficulty in generating antibodies against these nonimmunogenic fungal metabolites. Physicians can therefore only rely on general detoxification procedures such as gastric lavage, plasma exchange, or hemodialysis, to remove the toxins from the blood circulation once they have been ingested. The development of a drug that is able to sequester such ionophoric cyclodepsipeptides is thus urgently needed. In that regard, artificial receptors targeting these toxins might provide an answer to the aforementioned problems.

Many synthetic receptors have been developed for ligands such as anions,[13] cations,[14] saccharides,[15] small peptides, and even large entities such as fullerene[16] or entire proteins.[17,18] Yet despite these efforts, some ligands, including, e.g., medium-sized peptides, have remained unexplored. Indeed, most synthetic receptors for peptide-related structures reported to date only show affinity for di- or tripeptides[19−21] and the recognition of structures of intermediate size (between small peptides and large proteins), such as the cyclodepsipeptides described in this work, has proven particularly difficult. Moreover, no prior efforts toward the application of synthetic receptors in food safety and mitigation of food contamination risks have been deployed.

In an effort to fill this void, we previously described receptor **R1** (Figure 1)[22] which was able to recognize beauvericin with an affinity of 4.0×10^5 M^{-1} in $CHCl_3$. The design principle for receptor **R1** was based on two key features of the toxin, namely, its lipophilic nature and its ability to bind cations such as NH_4^+ and K^+. The incorporation of steroid side arms in the receptor allows interaction with the hydrophobic side chains of the toxin, while the protonated amine functionality connected to the central part of the carbazole linker mediates the ionophoric interaction. Due to the presence of the fluorogenic carbazole moiety in close proximity to the protonated amine, binding of BEA could be monitored via fluorescence measurements. However, for receptor **R1** to be truly applicable as an antidote, some caveats still remain. The most prominent one resides in the rather lengthy synthesis (12 steps), in which certain steps caused problems during early scale-up attempts.

In this work, we improved on our initial design by developing receptor **R2** (Scheme 1), which can be synthesized in fewer steps and on a larger scale. Additionally, a series of receptor analogues featuring varying cavity sizes and different hydrophobic moieties were prepared to probe the impact of such changes on the selectivity and affinity for ionophoric toxins, which themselves have different sizes. To explore possible applications of the synthetic receptors, immobilization of the most promising analogue on solid support was performed. This led to a strong retention of beauvericin, thus opening the possibility of using this construct for solid-phase extraction (SPE) in food sample pretreatment.

More importantly, we report on the application of the synthetic receptor as antidote against beauvericin (Figure 2).

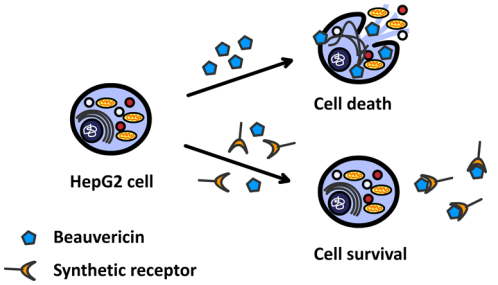

Figure 2. Use of the synthetic receptor to prevent beauvericin-mediated cell death.

We show that addition of 10 equiv of receptor allows to significantly reduce beauvericin-induced cytotoxicity in HepG2 (liver carcinoma) cells using multiple cell assays. This is the first example showing the use of an artificial receptor to counteract food-borne ionophore toxicity in vitro.

RESULTS AND DISCUSSION

Synthesis of Receptor R2. The main hurdles in the synthetic route toward previously described receptor **R1** were related to the functionalization of the C_{23} end of the steroid side arms. We reasoned that receptor **R2** with ester functionalities at the C_{23} extremities would be more accessible synthesis-wise without compromising the binding with BEA (Scheme 1). The synthesis of **R2** started with the Fisher esterification of commercially available lithocholic acid **1**, followed by acylation of the C_3−OH using bromoacetyl bromide. Subsequent second-order nucleophilic substitution reaction with NaN_3 gave us steroid **3** in good yield. The carbazole fragment **5** was synthesized as described previously.[22] Briefly, alkylation of 2,7-dibromocarbazole **4** was followed by a Sonogashira reaction[23] using 2-methyl-3-butyn-2-ol. Removal of the 2-hydroxy-isopropyl protecting group using NaH in toluene yielded compound **5** in satisfactory yield. Subsequently, both fragments **3** and **5** were coupled via a copper-catalyzed alkyne−azide cycloaddition (CuAAC) using Fokin−Sharpless conditions.[24] Receptor **R2** was obtained after removal of the *tert*-butyloxycarbonyl (Boc)-group using 4 M HCl in dioxane.[25]

The synthesis of **R2** involves only eight steps, which is considerable less than the 12 steps that were necessary for receptor **R1**. Moreover, the modular nature of the synthetic route depicted in Scheme 1 enables the straightforward generation of a variety of receptor analogues (vide infra). Before embarking on that journey, the affinity of receptor **R2** for BEA was assessed.

Determination of the Binding Affinity of Receptor R2. From the many techniques that are available for the determination of binding constants, fluorescence titration has proven to be particularly useful. This principle has been used by us before for receptor **R1**, in which case binding with BEA resulted in a pronounced fluorescence increase of the blue carbazole emission at 373 and 389 nm in $CHCl_3$.

Given the structural similarity between receptor **R1** and **R2**, we used the same methodology in this work to asses if receptor

DOI: 10.1021/acs.joc.9b01665
J. Org. Chem. XXXX, XXX, XXX−XXX

Scheme 1. Synthetic Route toward Receptor R2

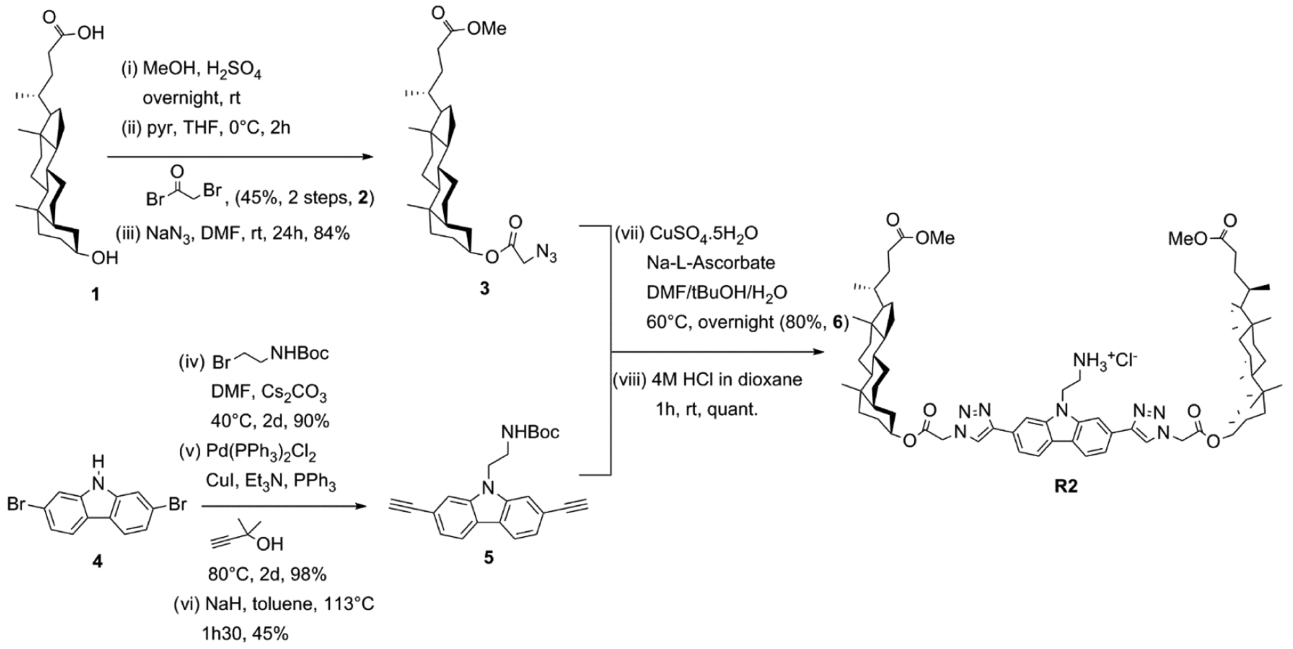

R2 is still capable of binding BEA with reasonable affinity. It is worth noting that the choice of excitation wavelength (λ_{ex}) for the titration is important. A common mistake in fluorescence titration is the negligence of the inner filter effect.[26] Briefly, if the added guest (e.g., BEA) absorbs at the excitation or emission wavelength, a decrease in emission intensity would be observed, which is unrelated to complex formation. This can result in misinterpretation of the results. A UV−vis experiment with BEA showed that this toxin absorbs considerably below 300 nm. However, above this value, the absorption (hence the inner filter effect) is negligible [Figure S1 in the Supporting Information (SI)]. This explains why 329 nm (n → π^* transition) was used as λ_{ex} and not the 250 nm region ($\pi \rightarrow \pi^*$ transition).

As shown in Figure 3, addition of BEA to **R2** in $CHCl_3$ resulted in an increase of the carbazole emission, similar to what has been observed before for **R1**. An association constant of 1.1×10^5 $M^{-1} \pm 4.5 \times 10^4$ [$K_a \pm$ standard deviation (SD)] was obtained, based on the mean of three independent titrations. This value was determined by fitting the fluorescence titration data at 389 nm to a theoretical binding isotherm for a 1:1 binding model.[22]

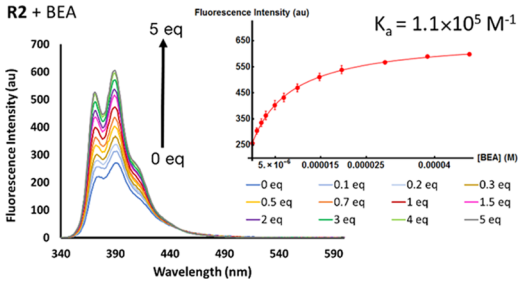

Figure 3. Fluorescence titration of 0−5 equiv BEA to 10 μM receptor **R2** in $CHCl_3$ using λ_{ex} = 329 nm. The inset shows the mean fluorescence intensity of **R2** at 389 nm as a function of added BEA concentration. The mean and standard errors at each titration point were calculated based on three independent titrations. Data points were fitted to a 1:1 stoichiometry (red line). See Figure S2 in the SI for a larger representation of the inset graph.

The observed complexation between **R2** and beauvericin is as expected, best explained considering a 1:1 binding stoichiometry. Indeed, when the titration data were fitted to a 2:1 or 1:2 host−guest stoichiometry,[27,28] no proper fit could be obtained (data not shown).

To provide further evidence for the binding between BEA and **R2**, we explored the possibility of using NMR titration and isothermal titration calorimetry (ITC). Both techniques require concentrations in the millimolar range. However, under such conditions, aggregation of the receptor in $CHCl_3$ was observed, which prevented comparison with the fluorescence titration data. As fluorescence titration can be performed at micromolar concentrations (UV−vis experiments showed that **R2** followed the Beer−Lambert law in this concentration range (data not shown)). Although receptor **R2** is soluble in dimethylformamide (DMF)-d_7, the added value of a NMR titration in this solvent is questionable. DMF, being a so-called dipolar aprotic solvent, will interact strongly with the ammonium cation of the receptors, which is, at the same time, vital for binding to the toxin. As such, data obtained in DMF cannot be compared with the fluorescence titration performed in $CHCl_3$. Therefore, other methods were considered to further support the binding of **R2** with BEA (vide infra SPE experiments and cell toxicity assays).

We have previously shown[22] that titration of the carbazole fragment alone, without any steroid side arms, yielded a 1000-fold lower binding affinity for BEA compared to receptor **R2** (Figure S3 in SI). On the other hand, when the Boc-protected receptor was tested, no change in fluorescence intensity was observed upon BEA addition (Figure S4 in SI). Taken together, these results indicate that both the ammonium functionality and the hydrophobic cavity generated by the steroid side arms are required for high-affinity binding and sensing of beauvericin. This observation was also confirmed by the application experiments reported in this work (SPE experiments and use of receptor **R2** as antidote, vide infra).

DOI: 10.1021/acs.joc.9b01665
J. Org. Chem. XXXX, XXX, XXX−XXX

The fourfold lower binding affinity of **R2** for BEA compared to **R1**, as determined using fluorescence titration, is somewhat surprising, considering that the only difference between both receptors lies in the C_{23} extremity. A possible explanation might be that the large bromine atoms in **R1** induce a conformational change in the receptor, which is favorable for the interaction with beauvericin. Nevertheless, the shorter synthesis of **R2** and its scalability outweigh the fourfold lower affinity. Moreover, certain solid-phase extraction (SPE) applications (vide infra) do not necessarily require high-affinity binders because the lower affinity can be compensated for by using an excess of immobilized receptor.

Variation of Cavity Size and/or Hydrophobic Moiety. The discovery that receptor **R2** has a fourfold lower affinity than **R1** prompted us to investigate if it would be possible to synthesize analogues of **R2** with higher affinity. As shown in Figure 4, in principle, the cavity sizes of receptors **R1** and **R2**

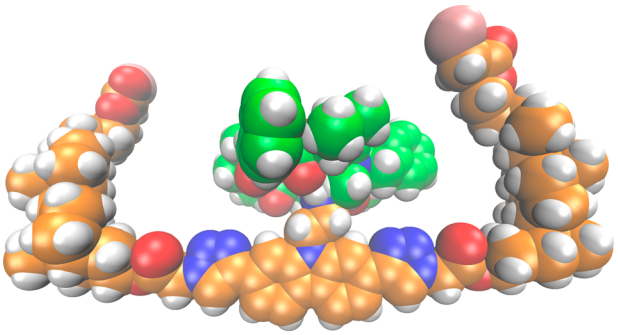

Figure 4. Visual representation of receptor **R1** (orange) and BEA (green) using visual molecular dynamics, illustrating the large cavity size. The same applies to **R2** (not shown).

are considerably large when taking the volume of BEA into account. Given our efficient and modular synthesis route for **R2**, variation of the cavity size was considered as a way to increase the affinity for BEA.

Synthesis of an alternative steroid fragment **9** (Scheme 2) featuring a shorter C_3 chain started with the Fisher esterification of lithocholic acid **1**, followed by oxidation of

Scheme 2. Synthetic Route toward Steroid Fragment 9

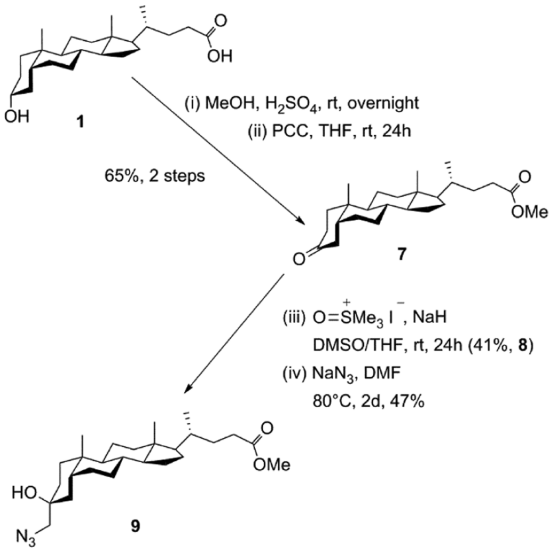

the secondary alcohol with PCC, yielding the corresponding ketone **7** in 65% yield (over two steps). The nucleophilic attack of the bulky sulfur ylide at the equatorial position resulted in the formation of the corresponding epoxide in a modest 41% yield,[29] which was ring-opened with NaN_3.

Building blocks **3** (Scheme 1) and **9** (Scheme 2) are both based on the lithocholic acid precursor that contains a *cis*-decalin ring fusion, responsible for its concave inner surface. Although this has usually been one of the reasons why this molecule is considered as scaffold for synthetic receptors, we were wondering if substitution with a hydrophobic moiety containing a *trans*-decalin system would influence the binding affinity with the ionophoric toxins.

An example of such *trans*-decalin scaffold is abietic acid, which is isolated from resin or conifer extracts. Multiple derivatives with interesting biological activity have been synthesized starting from this natural product.[30] Additionally, being a chiral building block, it has been employed as ligand for the Zn-catalyzed enantioselective Friedel–Crafts alkylation of *N*-methylindoles[31] and as chiral solvating agent for NMR analysis.[32] Yet, its use as a scaffold for synthetic receptors seems to be limited.[33]

The synthetic route toward abietic acid-based building block **15** follows a similar path to that described for its litocholic acid counterpart (Scheme 3). Hence, acylation of commercially

Scheme 3. Synthetic Route toward Abietic Acid-Based Fragment 15

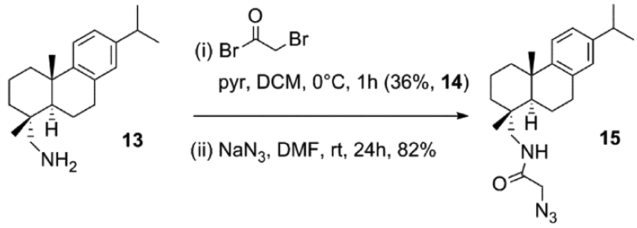

available dehydroabietylamine **13** with bromoacetyl bromide was followed by substitution with NaN_3, which yielded the desired azido-derivative **15** in 30% yield (two steps).

Having synthesized three different azido-functionalized building blocks (**3**, **9**, and **15**), coupling to carbazole moiety **5** via a CuAAC reaction was performed (Figure 6). As described earlier, reaction of steroid fragment **3** with carbazole **5** gave the receptor with the largest cavity size (**R2**). Interestingly, when conducting the CuAAC reaction using 2.5 equiv of the alternative steroid fragment **9**, mainly the monosubstituted reaction product was obtained. This difference in reactivity might be due to the closer proximity of the azide to the steroid skeleton in compound **9**, thereby rendering the azide more sterically crowded. The obtained monosubstituted derivative allows the synthesis of asymmetric receptor analogues. Hence, coupling of 2.5 equiv **9** followed by a second CuAAC reaction with fragment **3** gave a receptor with an intermediate cavity size (**R3**), while coupling of **9** in excess (8 equiv) yielded receptor **R4**, which has the smallest cavity size. Finally, the CuAAC reaction using abietic acid-based fragment **15** yielded receptor **R5**.

Binding Affinity of the Receptor Analogues for the Different Ionophores. With the different receptor analogues at hand, we were keen to investigate how changing the cavity size (receptors **R2**–**R4**) or using the abietic acid scaffold

DOI: 10.1021/acs.joc.9b01665
J. Org. Chem. XXXX, XXX, XXX–XXX

(receptor **R5**) would influence the binding affinity for ionophoric toxins, which themselves have different sizes. While our previous endeavors were mainly directed toward the binding of beauvericin or valinomycin (VAL), in this work, we decided to expand the number of tested ionophores. Therefore, enniatin B, the enniatin subtype most frequently found in contaminated food (vide supra), was also included to obtain a clearer picture on the relationship between receptor structure and affinity for a particular toxin. Valinomycin (VAL) was tested because of its strong analogy to BEA. Both are cyclodepsipeptides, able to bind NH_4^+. Yet their size is significantly different (Figure 5). To determine the binding

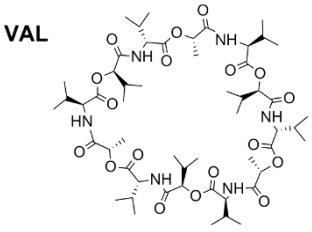

	molecular weight
ENN B	640 g/mol
BEA	783 g/mol
VAL	1111 g/mol

Figure 5. Chemical structure of valinomycin (left) and tabulation of the molecular weights of the different ionophores (right).

affinity, fluorescence titration was used (Figures S5–S8 in the SI), as already described above for receptor **R2**. The resulting association constants for BEA and ENN B are depicted in Figure 6 (K_{BEA} and K_{ENN}, respectively).

A couple of interesting observations can be made when looking at the experimental data. Upon decreasing the cavity size, the binding affinity for BEA increased, while this was not the case for the smaller toxin ENN B. Rather unexpectedly, the highest affinities were obtained with the abietic acid-based receptor **R5**, which showed an affinity of 1.6×10^6 M^{-1}. This is a 10-fold increase in binding affinity for BEA compared to receptor **R2**. However, the higher affinity came at the cost of completely losing the selectivity between the individual ionophores.

These results seem to indicate that the use of a scaffold containing the *trans*-decalin system is clearly advantageous compared to one containing a cis-fused ring (e.g., lithocholic acid), when higher affinities are required. Finally, none of the receptors showed appreciable interaction with the larger ionophore valinomycin, which is in line with our previous observation for receptor **R1**.[22] For further applications, the more complicated synthesis of receptors **R3** and **R4** is not outweighted by the small increase in affinity compared to receptor **R2**. Abietic acid-based receptor **R5**, on the other hand, does show a significantly higher affinity, but the loss of selectivity for the different ionophores makes it less attractive. Taking all of the above into account, receptor **R2** was chosen for subsequent experiments aimed at exploring its use in potential applications.

Synthesis and Immobilization of the Receptor for Solid-Phase Extraction (SPE). Currently, analysis of mycotoxins is generally achieved using liquid chromatography–tandem mass spectrometry (LC–MS/MS), through direct injection of the sample in a diluted fashion without any pretreatment step. Even though this can be done for simple food matrices such as pasta, bread, rice, etc., the analysis of complex food samples is far more challenging. Because of the complexity of the matrix in the latter, sample pretreatment is usually required. This is mainly performed using SPE cartridges that contain a solid support with affinity for the analyte. After addition of a sample to the cartridge, the analyte will be retained more effectively on the solid support compared to matrix components. By using an appropriate eluent (eluent 1 in Figure 7), the interfering matrix can be eluted, while the analyte remains bound to the sorbent. Subsequently switching toward a more competitive eluent (eluent 2) allows isolation of the analyte.

For most mycotoxins, highly specific SPE cartridges exist based on antibodies. However, due to the lack thereof for BEA and ENN, such cartridges are unavailable for these toxins. Therefore, only nonselective SPE cartridges have been used, such as C18. Recently, also a graphitized carbon black sorbent

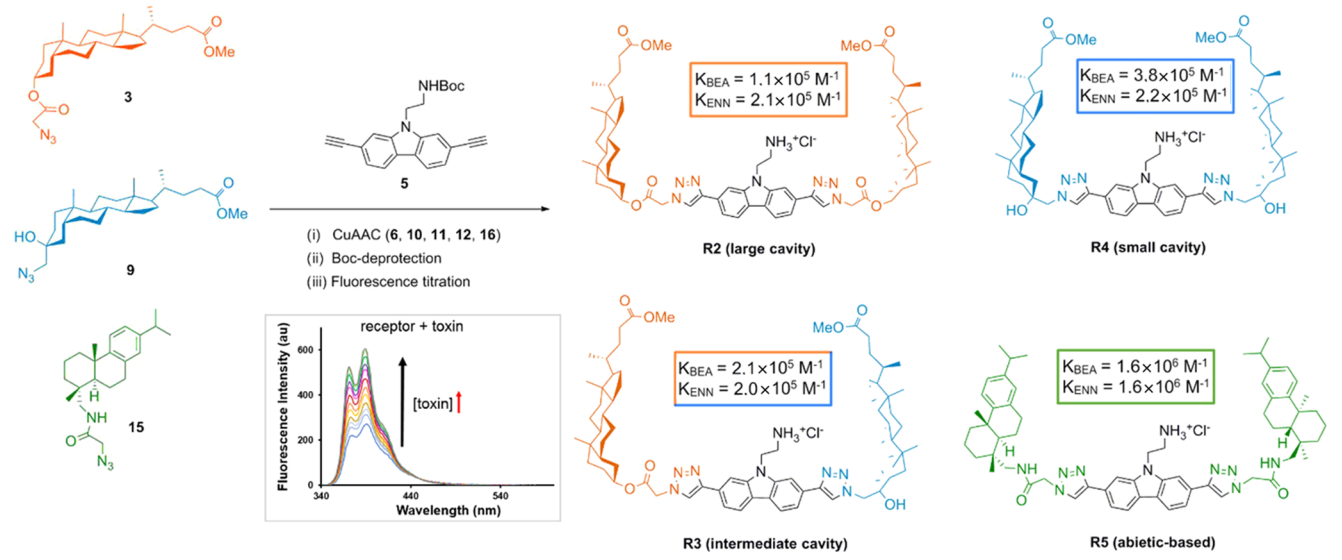

Figure 6. CuAAC reaction of carbazole **5** with different azido-functionalized hydrophobic scaffolds (**3**, **9**, and **15**) gave intermediates **6**, **10**–**12**, and **16** (structures not shown). Subsequent Boc deprotection yielded receptors **R2**–**R5**. The association constants of each receptor for BEA (K_{BEA}) and ENN B (K_{ENN}) were determined using fluorescence titration (λ_{ex} = 329 nm) in $CHCl_3$ (mean of three independent titrations). Standard deviation values for each titration can be found in Table S2 (SI).

DOI: 10.1021/acs.joc.9b01665
J. Org. Chem. XXXX, XXX, XXX–XXX

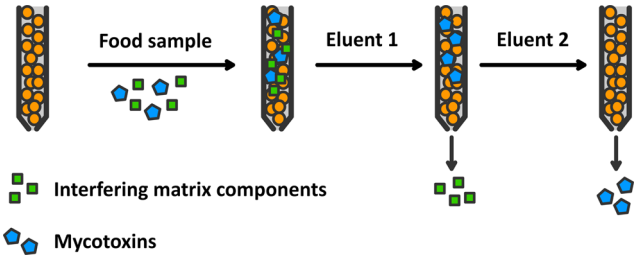

Figure 7. Illustration of the principle behind SPE.

has been employed for the extraction of ENN and BEA from human urine and plasma.[34]

Our goal was to synthesize an analogue of **R2** containing carboxylic acid handles rather than esters (**R6**) for coupling onto 3-aminopropyl-functionalized silica (Scheme 4A). This would potentially endow the sorbent material with affinity for BEA. Such material could find practical use in the solid-phase extraction of ionophoric toxins.

Scheme 4. Immobilization of R6 onto Solid Support (A) and Acetylation of the Resin (B)

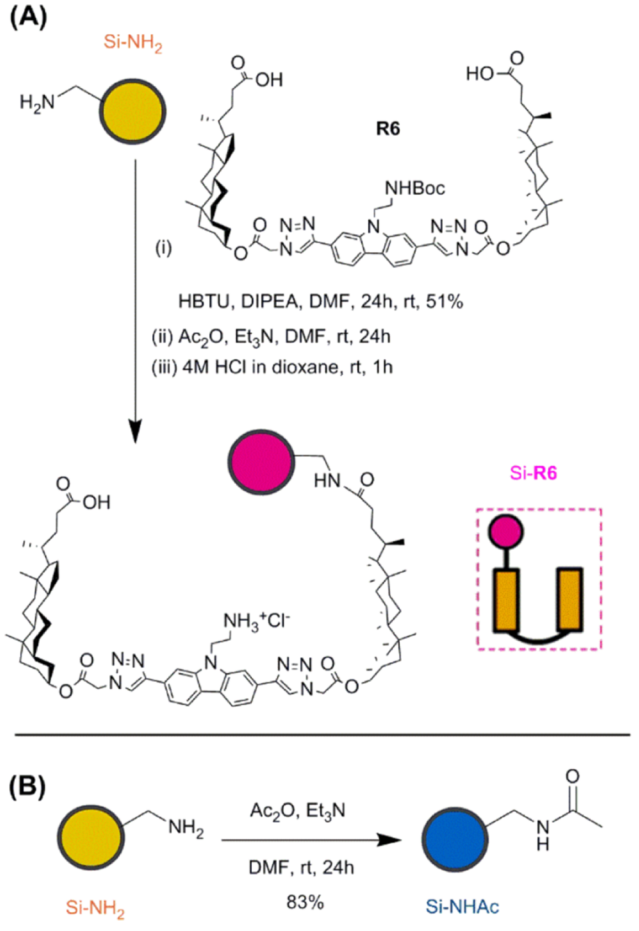

The synthesis of **R6** was accomplished via a route analogous to the one described in Scheme 1 (see Experimental Section). Subsequent immobilization on 3-aminopropyl-functionalized silica (Si-NH_2) using 2-(1*H*-benzotriazol-1-yl)-1,1,3,3-tetramethyluronium hexafluorophosphate (HBTU) and *N*,*N*-diisopropylethylamine (DIPEA) proceeded in 51% yield (Scheme 4A). Indeed, red coloration of the beads after the 2,4,6-trinitrobenzenesulfonic acid (TNBS) test indicated incomplete coupling. Therefore, a capping step with Ac_2O and Et_3N was performed to block any residual free amine on the resin. The successful capping was confirmed by the TNBS test.

Next to the immobilization of **R6** (Si-**R6**), acetylated resin (Si-NHAc) (Scheme 4B) and 3-aminopropyl base resin (Si-NH_2) were evaluated as controls. While the former should only feature background absorption related to the resin material, the latter can show nonselective ionophoric interactions with the toxin.

To assess which of the three resins was most effective at retaining BEA, each resin was incubated overnight with 3 mL of a 100 nM BEA solution in hexane. The next day, the solvent was removed (=rest fraction) and the resin was subjected to a gradient elution (hexane/EtOAc) (Figure 8). The beauvericin concentration in each collected fraction was determined via LC−MS/MS.[35]

It is to be expected that the stronger the binding between the resin and BEA, the more polar the eluent must be to disrupt this interaction. As shown in Figure 8 (bottom left), a pronounced difference between the resins could be observed. The toxin is retained far more efficiently on the resin containing immobilized **R6** (pink) compared to the acetylated (blue) or amino-functionalized resin (yellow). The observed retention capabilities of the resins increase in the order: Si-NHAc < Si-NH_2 < Si-**R6**. This corresponds to the expected interaction strength between the modified solid supports and the toxin (vide supra).

More importantly, our immobilized receptor proved to be superior in retaining BEA compared to Si-NH_2, which can be attributed to a combination of the hydrophobic cavity size with the ammonium functionality interacting in concert with the toxin. As such, this SPE experiment further validates the important contribution of the receptor cavity with respect to toxin binding and is consistent with the 1000-fold lower affinity measured for the individual carbazole fragment compared to the receptor, as mentioned earlier. Moreover, it is worth noting that BEA is retained poorly on the acetylated resin, which indicates that hydrophobic interactions alone are not sufficient for binding the toxin. This is in line with our observation that when the amine of the receptor is Boc-protected (hence only hydrophobic interactions are available for toxin binding), no change in fluorescence intensity is observed (vide supra). The fact that Si-**R6** is able to retain BEA provides further evidence for the specific interaction between our synthetic receptor and BEA, in accordance with the obtained fluorescence titration data (vide supra).

The same fluorescence titration experiments also revealed that receptor **R2** did not bind the larger ionophore valinomycin. Upon using a 100 nM VAL solution, interestingly, all three resins behave similarly with respect to VAL retention (Figure 8, bottom right), which is in strong contrast with the results obtained for BEA. The selectivity observed for **R2** in fluorescence titration is thus maintained upon its immobilization onto solid support. These experiments independently confirm the observations made during the fluorescence titrations regarding the affinity of the receptor for BEA. At the same time, they constitute a first step toward the development of a selective SPE cartridge for beauvericin.

Application of R2 in Cell Cultures. Although our endeavors in developing synthetic receptors for ionophoric toxins were initially driven with analytical applications in mind (e.g., their use in solid-phase extraction), it became tempting

DOI: 10.1021/acs.joc.9b01665
J. Org. Chem. XXXX, XXX, XXX−XXX

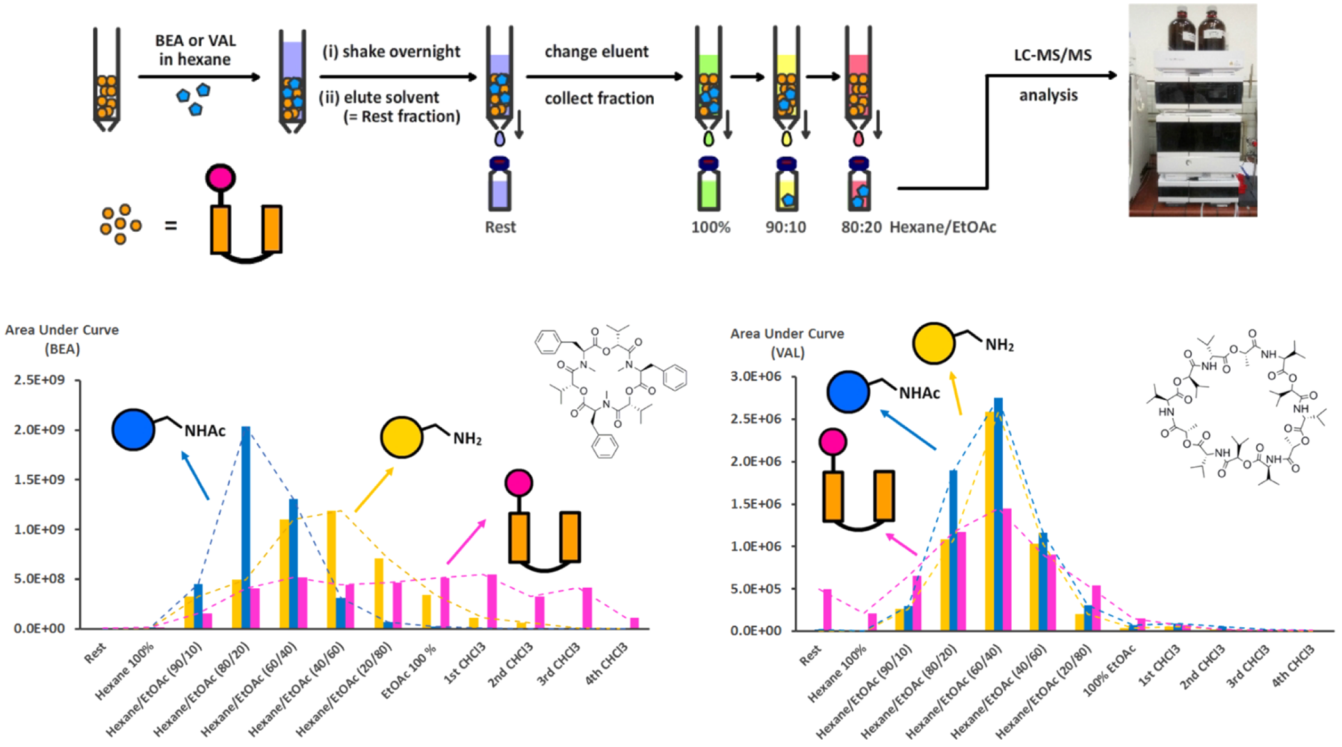

Figure 8. Illustration of the SPE experimental setup (top). Gradient elution of BEA (bottom left) and VAL (bottom right) using acetylated resin (blue), 3-aminopropyl-functionalized silica resin (yellow) modified with **R6** (pink). The area under the curve of the most abundant BEA or VAL fragment ion in each collected fraction (LC−MS/MS) is shown on the vertical axis.

to consider if the recognition capabilities of receptor **R2** toward BEA could be used in a medicinal/pharmaceutical setting. By binding beauvericin, **R2** might be able to act as antidote and prevent cell death. Currently, only one procedure has been reported in the literature, in which the authors use the antioxidant resveratrol to counteract the toxicity of beauvericin in vitro.[36] However, this method only tackles one of the downstream effects of BEA toxicity (e.g., reactive oxygen species (ROS) production) and not the actual interaction of BEA with host cells. This interaction goes deeper and beyond ROS production. Work by Jow and co-workers has shown that addition of 10 μM BEA to human leukemia cells (CCRF-CEM) induced the release of cytochrome *c* from mitochondria, which in turn causes apoptosis via the caspase-3 pathway.[10] Evidence has also been put forward for the binding of beauvericin to DNA[37] and its ability to inhibit the enzyme acyl-CoA/cholesterol acyltransferase.[38] By sequestering the toxin using a synthetic receptor, all downstream pathways would be inhibited, not only ROS production.

As a proof of principle, we investigated if a mixture of BEA and **R2** would be less toxic in vitro compared to BEA alone. For these experiments, human liver carcinoma (HepG2) cells were chosen based on earlier reports that BEA accumulates in the liver when administered to mice.[11] Cell viability was assessed using three complementary assays. The first assay is the 3-(4,5-dimethylthiazol-2-yl)-2,5-diphenyltetrazoliumbromide (MTT) assay, which is based on the reduction of MTT by viable cells to the purple dye formazan.[39] It is worth noting that although this assay is often interpreted as a cell viability assay, it is actually a metabolic activity assay. If a compound is employed which is nontoxic but inhibits the reduction of MTT to formazan, the assay would incorrectly be interpreted as a decrease in viable cell count.

Hence, in this work, we conducted two additional assays to validate the results obtained with MTT, namely, the neutral red (NR) and sulforhodamine (SRB) assay. The NR assay is based on the accumulation of the dye neutral red in lysosomes of living cells, which is linearly dependent on the number of viable cells.[40] The SRB assay, on the other hand, relies on the binding of sulforhodamine B to proteins and, as such, is a measure of protein content (e.g., cell density, unless the compound under study severely alters protein expression).[41] While none of these assays are fail-safe on their own as a measure of cell viability, using all three of them in concert improves the reliability of the interpretation.

In a first experiment, different quantities of BEA were dissolved in DMF, followed by addition of growth medium to obtain solutions containing 1% DMF and BEA concentrations ranging from 0.2 to 30 μM. This solvent was chosen due to its solvating capability toward both the toxin and the receptor. Control experiments showed that 1% DMF is well tolerated by the cells while higher concentrations are cytotoxic (data not shown). The three assays clearly showed signs of toxicity after 24 h incubation of HepG2 cells with beauvericin, starting at 2.5 μM BEA (Figures S10 and S12 in the SI). At 15 μM, complete cell death was observed, which is consistent with what has been reported by others on the same cell line.[42]

Before performing the toxicity assays of receptor **R2**−beauvericin mixtures, the toxicity of receptor **R2** alone was investigated. Indeed, if the receptor would be highly toxic on its own, its use as an antidote would be jeopardized. The results obtained showed no toxicity of **R2** in any of the deployed assays (MTT, NR, and SRB), even at the highest dose tested of 200 μM (Figures S14 and S16 the in SI).

DOI: 10.1021/acs.joc.9b01665
J. Org. Chem. XXXX, XXX, XXX−XXX

Based on the above results, we decided to prepare mixtures of 5 μM BEA in combination with 1 or 10 equiv **R2**, while maintaining the total DMF concentration constant. As shown in Figure 9, addition of 1 equiv **R2** to 5 μM BEA was not sufficient to significantly reduce the toxicity observed visually under the light microscope (Figure 9B vs Figure 9C).

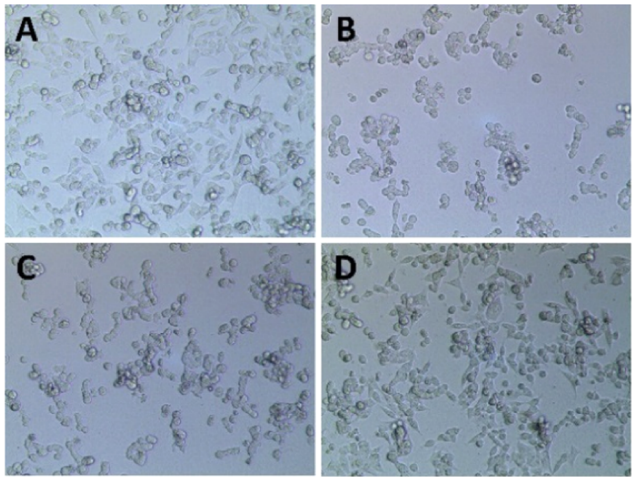

Figure 9. Image under the light microscope of HepG2 cells after 24 h incubation at 37 °C with (A) 1% DMF, (B) 5 μM BEA, (C) 5 μM BEA + 1 equiv **R2**, and (D) 5 μM BEA + 10 equiv **R2**.

However, addition of 10 equiv **R2** clearly led to a lower toxicity (Figure 9D) compared to cells treated with 5 μM BEA alone (Figure 9B). This was also confirmed with the MTT, SRB, and NR assay (Figures S18 and S20 in the SI). A similar observation was made in the experiments using 2.5 μM BEA (SI).

More interestingly, a mixture of 10 equiv **R2** and 15 μM BEA still showed a cell survival rate of ±60% in the NR assay. This is in strong contrast to those cells that were treated with 15 μM BEA alone, which causes complete cell death (Figure 10). These results demonstrate the remarkable ability of **R2** to protect cells from BEA-mediated cytotoxicity, which was also confirmed with the SRB assay (Figure S20 in the SI).

It is not entirely surprising that an equimolar mixture of **R2** and BEA at 15 μM concentration only has a reduced protecting effect on the cells, having determined that the stability constants of the 1:1 complexes are in the range of 10^5–10^6 M^{-1}. Indeed, under those conditions, a great extent of the ionophore is still free in solution. The protecting effect of **R2** increases as the number of equivalents is increased. This result can be considered a direct consequence of the reduction of free ionophore in solution. Furthermore, also nonselective binding of **R2** to compounds present in the complex cell medium (e.g., serum albumin) could play a role. It is worth noting that during the course of the experiment, fetal bovine serum was always present. While we could have opted to avoid the presence of serum during the treatment of the cells with the receptor–toxin mixtures, we feel that performing the experiments with this complex additive present is more representative of the real-life situation. Moreover, considering the fact that the affinity of receptor **R2** for BEA was in the 10^5 M^{-1} range, addition of only 1 equiv **R2** is not sufficient to bind all of the toxin in solution. As such, the amount of free toxin is still high enough to cause cytotoxicity. Upon addition of an excess receptor, the concentration of free toxin decreases, which in turn reduces the observed toxicity.

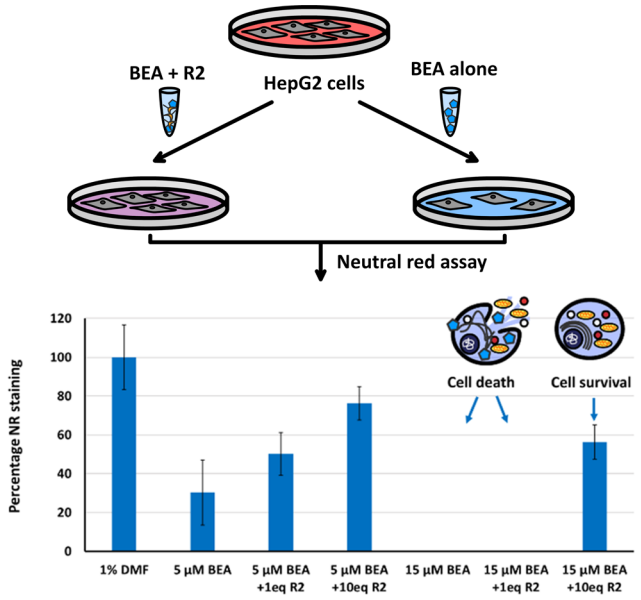

Figure 10. Results of the NR assay after 24 h incubation of HepG2 cells at 37 °C with different concentrations of beauvericin alone or in combination with 1 or 10 equiv receptor **R2**. The error bars represent the relative SD value.

Finally, as a control, the Boc-protected derivative of **R2** was also tested, which lacks the ionophoric interaction with the toxin. In this case, no decrease in cytotoxicity was notable (Figure S23 in the SI), thereby highlighting the importance of the ammonium functionality in **R2**. This is in accordance with the observation that the Boc-protected receptor does not show any increase in fluorescence intensity upon addition of beauvericin (vide supra).

It is important to stress that if receptor **R2** would not be able to bind BEA, a reduction in cytotoxicity should not be observed. Likewise, during the SPE experiments, the strong retention of BEA by the immobilized receptor confirms the binding event. While one might want to confirm the binding affinity with more classical techniques such as ITC or NMR, solubility limitations prevented their use (vide supra). Both the fact that the receptor is able to retain BEA in an SPE retention experiment and the observation that the receptor reduces beauvericin-induced cytotoxicity provide clear and independent evidence of the affinity and selectivity of the receptor for beauvericin.

CONCLUSIONS

In summary, we here report on an improved synthetic route toward an artificial receptor with affinity for beauvericin (8 steps compared to 12 steps reported previously). The binding affinity of the receptor for beauvercin was confirmed by three independent methods: fluorescence titration, SPE retention experiments, and cell assays. Additionally, the highly optimized convergent synthetic route was further exploited in a versatile way to obtain a series of new receptor analogues with varying cavity sizes or hydrophobic moieties, all of which were tested for affinity against three different ionophoric toxins. While receptor cavity size had a moderate impact on the affinity, the use of an abietic-based scaffold instead of lithocholic acid increased the binding affinity considerably, albeit at the cost of

DOI: 10.1021/acs.joc.9b01665
J. Org. Chem. XXXX, XXX, XXX–XXX

selectivity. The obtained data allow to rationalize and guide further design efforts.

Taking into account the widespread occurrence of beauvericin in food samples and the fact that a recent European Food Safety Authority report[43] urges the acquisition of more data to evaluate the chronic toxicity of beauvericin, improved detection methods for this toxin are urgently needed. To date, there is a total lack of SPE cartridges that are selective for beauvericin. This limits the possibility of detecting the toxin in complex food samples, which require a pretreatment step with SPE. In this context, we immobilized the most promising receptor on solid support, which led to a strong retention of beauvericin in a solid-phase extraction setup. This yielded the first sorbent material with affinity for beauvericin with the potential to discriminate between BEA and other ionophoric cyclodepsipeptides such as valinomycin. As such, the developed material can be valuable for future application in the capture and detection of beauvericin in complex food samples.

Finally, we showed for the first time that this type or artificial receptor can be used to reduce beauvericin-mediated cytotoxicity in HepG2 cells, thus paving the way toward its potential use as an antidote.

Future work will be aimed at shining light on the mechanism behind this protective effect. In addition, the differential response of each receptor analogue for the ionophoric toxins opens up the possibility of using this small receptor library in the development of a chemical nose sensor[44] for the detection of beauvericin and enniatins.

EXPERIMENTAL SECTION

General Information. Chemical shifts are reported in parts per million (ppm) using tetramethylsilane as an internal standard. All chemicals were purchased from Sigma-Aldrich with the exception of beauvericin, which was purchased from Fermentek, and 2,7-dibromocarbazole, which was purchased from TCI. Column chromatography was performed on 200 μm silica gel (Davisil, Grace Davison). Yields are reported for the isolated compounds. High-resolution mass spectrometry (HRMS) images were recorded on an Agilent 1100 series high-performance liquid chromatography connected to an Agilent 6220A time-of-flight high-resolution mass detector equipped with an electrospray ionization (ESI)/atmospheric-pressure chemical ionization multimode ionization source. Unless otherwise stated, ionization was performed in positive ESI mode. Infrared spectra were recorded on a PerkinElmer 1000 FTIR spectrometer equipped with a Pike ATR module.

Chemical Synthesis. *Methyl-3α-bromoacetoxy-5β-cholan-24-oate (**2**).* Lithocholic acid **1** (2.0 g, 5.5 mmol) was dissolved in 30 mL of MeOH, followed by addition of 0.4 mL of concentrated H_2SO_4. The mixture was stirred at room temperature (rt) overnight. The solvent was removed in vacuo, and the residue was dissolved in EtOAc. After washing with H_2O, the organic phase was evaporated, yielding the methyl ester as a white solid. The ester was dissolved without any further purification in 20 mL of dry tetrahydrofuran (THF), followed by addition of 4 equiv pyridine (1.8 mL, 22.1 mmol). The mixture was cooled to 0 °C, and bromoacetyl bromide (1.0 mL, 11.0 mmol, 2 equiv) was added, followed by stirring for 2 h at 0 °C. The mixture was poured in H_2O, extracted with dichloromethane (DCM), and the organic phase was evaporated in vacuo. The crude was dry-loaded onto 4 g of silica and purified via flash chromatography (eluent 95:5 hexane/EtOAc) yielding compound **2** as a white solid (1.3 g, 45%). ^{1}H NMR (400 MHz, $CDCl_3$) δ: 0.64 (s, 3H), 0.87−2.00 (m, 34H), 2.28 (m, 2H), 3.66 (s, 3H), 3.80 (s, 2H), 4.79 (m, 1H). $^{13}C\{^1H\}$ NMR (101 MHz, $CDCl_3$) δ: 12.2, 18.5, 21.0, 23.5, 24.4, 26.47, 26.56, 26.60, 27.2, 28.4, 31.19, 31.25, 32.1, 34.8, 35.1, 35.5, 36.0, 40.3, 40.6, 42.1, 42.9, 51.7, 56.2, 56.7, 76.8, 167.0, 174.9. HRMS m/z: calcd for $C_{27}H_{47}BrNO_4$ $[M + NH_4]^+$ 528.2683, found 528.2680.

*Methyl-3α-azidoacetoxy-5β-cholan-24-oate (**3**).* Compound **2** (1.3 g, 2.5 mmol) was dissolved in dry DMF, to which NaN_3 (963 mg, 14.8 mmol, 6 equiv) was added, followed by stirring at rt for 24 h. The mixture was poured in 150 mL of H_2O and extracted with EtOAc. The organic phase was concentrated in vacuo, and the crude was dry-loaded onto 4 g of silica. Purification via flash chromatography (eluent 90:10 hexane/EtOAc) yielded compound **3** as a white powder (987 mg, 84%). ^{1}H NMR (300 MHz, $CDCl_3$) δ: 0.65 (s, 3H), 0.80−2.04 (m, 35H), 2.29 (m, 2H), 3.67 (s, 3H), 3.83 (s, 2H), 4.84 (m, 1H). $^{13}C\{^1H\}$ NMR (75 MHz, $CDCl_3$) δ: 12.2, 18.4, 21.0, 23.5, 24.4, 26.5, 26.8, 27.2, 28.4, 31.19, 31.25, 32.3, 34.8, 35.1, 35.5, 36.0, 40.3, 40.6, 42.1, 42.9, 50.8, 51.7, 56.2, 56.7, 76.6, 168.0, 175.0. IR (ν_{max} in cm^{-1}): 2935, 2864, 2106, 1754, 1731. HRMS m/z: calcd for $C_{27}H_{47}N_4O_4$ $[M + NH_4]^+$ 491.3592, found 491.3601.

*Methyl (4R)-4-((3R,8S,9R,13S,14R)-3-(2-(4-(9-(2-((tert-Butoxycarbonyl)amino)ethyl)-7-(1-(2-(((3R,5R,8R,9S,10S,13R,14S)-17-((R)-5-methoxy-5-oxopentan-2-yl)-10,13-di- methylhexadecahydro-1H-cyclopenta[a]phenanthren-3-yl)oxy)-2-oxoethyl)-1H-1,2,3-triazol-4-yl)-9H-carbazol-2-yl)-1H-1,2,3-triazol-1-yl)acetoxy)-10,13-dimethylhexadecahydro-1H-cyclopenta[a]phenanthren-17-yl)pentanoate (**6**).* Compound **5** (synthesized as reported previously starting from 2,7-dibromocarbazole **4**)[22] (24 mg, 0.066 mmol) and compound **3** (78 mg, 0.166 mmol, 2.5 equiv) were dissolved in 4 mL of DMF, followed by addition of 6 mL of *t*BuOH. $CuSO_4{\cdot}5H_2O$ (33 mg, 0.132 mmol, 2 equiv) and Na-L-ascorbate (52 mg, 0.264 mmol, 4 equiv) were separately dissolved in 1 mL of H_2O each and added to the reaction mixture. The reaction was flushed under N_2 for 15 min and stirred at 60 °C overnight. The solvent was partially evaporated, and the residue was poured in a mixture of 80 mL of H_2O and 30 mL of EtOAc. The aqueous phase is extracted two more times with EtOAc. The collected fractions were evaporated, and the residue was dry-loaded onto 1 g of silica. Purification via flash chromatography (eluent 1:1 hexane/EtOAc) yielded compound **6** as a pink powder (69 mg, 80%). ^{1}H NMR (400 MHz, $CDCl_3$) δ: 0.64 (s, 6H), 0.87−2.00 (m, 78H), 2.28 (m, 4H), 3.63 (s + m, 8H), 4.54 (t, ^3J = 5.4 Hz, 2H), 4.72 (t, ^3J = 5.2 Hz, 1H), 4.87 (m, 2H), 5.20 (s, 4H), 7.67 (d, ^3J = 8.1 Hz, 2H), 8.02 (s, 4H), 8.09 (d, ^3J = 8.1 Hz, 2H). $^{13}C\{^1H\}$ NMR (101 MHz, $CDCl_3$) δ: 12.2, 18.5, 21.0, 23.5, 24.4, 26.5, 26.7, 27.2, 28.4, 28.5, 31.18, 31.24, 32.3, 34.8, 35.1, 35.5, 36.0, 40.3, 40.6, 42.1, 42.9, 51.4, 51.7, 56.1, 56.6, 77.3, 106.2, 117.8, 120.9, 121.4, 123.0, 128.5, 141.7, 149.2, 166.0, 175.0. HRMS m/z: calcd for $C_{77}H_{109}N_8O_{10}$ $[M + H]^+$ 1305.8261, found 1305.8272.

*2-(2-(1-(2-(((3R,5R,8R,9S,10S,13R,14S)-17-((R)-5-Methoxy-5-oxopentan-2-yl)-10,13-dimethylhexadecahydro-1H-cyclopenta[a]-phenanthren-3-yl)oxy)-2-oxoethyl)-1H-1,2,3-triazol-4-yl)-7-(1-(2-(((3R,8S,9R,13S,14R)-17-((R)-5-methoxy-5-oxopentan-2-yl)-10,13-dimethylhexadecahydro-1H-cyclopenta[a]phenanthren-3-yl)oxy)-2-oxoethyl)-1H-1,2,3-triazol-4-yl)-9H-carbazol-9-yl)ethan-1-amonium Chloride (**R2**).* To compound **6** (6.9 mg, 0.005 mmol), 2 mL of 4 M HCl in dioxane was added. The mixture was stirred at rt for 1 h. Evaporation of the solvent yielded receptor **R2** quantitatively as a pink powder. ^{1}H NMR (400 MHz, DMF-d_7) δ: 0.67 (s, 6H), 0.84−2.01 (m, 70H), 2.32 (m, 4H), 3.64 (s, 6H), 3.68 (m, 2H), 4.83 (m, 2H), 5.10 (t, ^3J = 6.6 Hz, 2H), 5.60 (s, 4H), 7.93 (d, ^3J = 7.8 Hz, 2H), 8.29 (d, ^3J = 7.8 Hz, 2H), 8.56 (s, 2H), 8.97 (s, 2H), 9.05 (s, 3H). $^{13}C\{^1H\}$ NMR (101 MHz, DMF-d_7) δ: 12.6, 18.9, 21.7, 23.8, 25.0, 27.2, 27.4, 27.9, 29.0, 32.0, 33.0, 36.8, 39.8, 41.0, 41.3, 42.7, 43.6, 44.6, 51.9, 56.9, 57.3, 61.9, 69.0, 71.9, 72.0, 73.7, 77.1, 107.4, 118.1, 121.7, 123.6, 124.2, 130.2, 142.7, 149.0, 168.1, 175.0. HRMS m/z: calcd for $C_{72}H_{101}N_8O_8$ $[M + H]^+$ 1205.7737, found 1205.7736.

*Methyl-3-oxo-5β-cholan-24-oate (**7**).* Lithocholic acid **1** (1 g, 2.65 mmol) was dissolved in 30 mL of MeOH. Concentrated H_2SO_4 (0.4 mL) was injected, and the mixture was stirred overnight at rt. After evaporation of the solvent, the residue was dissolved in 40 mL of EtOAc and washed with H_2O. The organic phase was evaporated, and the crude was used without further purification. The obtained methyl ester was dissolved in 15 mL of dry THF, followed by addition of 2.9 g of pyridinium chlorochromate (13.25 mmol, 5 equiv). The mixture was stirred at rt for 24 h. The solvent was removed in vacuo, and the

DOI: 10.1021/acs.joc.9b01665
J. Org. Chem. XXXX, XXX, XXX−XXX

residue was dry-loaded onto 3 g of silica. Purification via flash chromatography (eluent 90:10 hexane/EtOAc) yielded compound **7** as a white powder (672 mg, 65% in two steps). ^{1}H NMR (400 MHz, $CDCl_3$) δ: 0.67 (s, 3H), 0.91 (d, ^3J = 6.5 Hz, 3H), 1.00 (s, 3H), 1.03−2.41 (m, 28H), 2.68 (t, ^3J = 14.3 Hz, 1H), 3.65 (s, 3H). ^{13}C{^{1}H} NMR (101 MHz, $CDCl_3$) δ: 12.2, 18.5, 21.4, 22.9, 24.3, 26.0, 26.8, 28.4, 31.14, 31.2, 35.1, 35.5, 35.7, 37.2, 37.4, 40.2, 40.9, 42.5, 42.9, 44.5, 51.7, 56.1, 56.6, 174.9, 213.6. IR (ν_{max} in cm^{-1}): 2925, 2868, 2850, 1735, 1711. HRMS *m*/*z*: calcd for $C_{25}H_{44}NO_3$ [M + NH_4]$^+$ 406.3316, found 406.3329.

*(3S)-Spiro[24-methyl-5β-cholan-24-oate-3,2′-oxirane] (**8**).* Trimethylsulfoxonium iodide (1.1 g, 5.12 mmol, 1.5 equiv) and NaH (273 mg, 6.82 mmol, 2 equiv) were dissolved in 10 mL of dry dimethyl sulfoxide (DMSO). This mixture was stirred for 1 h at rt. Compound **7** (1.3 g, 3.41 mmol) dissolved in 5 mL of dry THF was added, and the resulting mixture was stirred at rt for 24 h. The mixture was poured into 100 mL of H_2O and extracted with DCM. The combined organic phases were evaporated in vacuo, and the crude was dry-loaded onto 3 g of silica. Purification via flash chromatography (eluent 90:10 hexane/EtOAc) yielded compound **8** as a white powder (565 mg, 41%). ^{1}H NMR (500 MHz, $CDCl_3$) δ: 0.66 (s, 3H), 0.78−2.00 (m, 32H), 2.29 (m, 3H), 2.61 (s, 2H), 3.66 (s, 3H). ^{13}C{^{1}H} NMR (126 MHz, $CDCl_3$) δ: 12.3, 18.5, 21.3, 23.6, 24.4, 26.4, 26.7, 28.33, 28.37, 31.19, 31.24, 33.7, 34.4, 34.8, 35.6, 35.8, 40.2, 40.4, 40.9, 43.0, 51.7, 53.8, 56.2, 56.8, 59.4, 174.9. HRMS *m*/*z*: calcd for $C_{26}H_{43}O_3$ [M + H]$^+$ 403.3207, found 403.3223.

*(3S)-Methyl-3-azidomethyl-3-hydroxy-5β-cholan-24-oate (**9**).* Compound **8** (142 mg, 0.35 mmol) was dissolved in 10 mL of dry DMF, followed by addition of 229 mg of NaN_3 (3.52 mmol, 10 equiv). The mixture was stirred at 80 °C for 2 days. The mixture was poured into 100 mL of H_2O and extracted with EtOAc, followed by evaporation of the organic phase in vacuo. The crude was purified via flash chromatography (eluent 50:48:2 DCM/hexane/EtOAc) yielding compound **9** as a white powder (73 mg, 47%). ^{1}H NMR (400 MHz, $CDCl_3$) δ: 0.64 (s, 3H), 0.90 (d, ^3J = 6.4 Hz, 3H), 0.94−2.00 (m, 32H), 2.28 (m, 2H), 3.24 (s, 2H), 3.66 (s, 3H). ^{13}C{^{1}H} NMR (101 MHz, $CDCl_3$) δ: 12.2, 18.4, 21.2, 23.8, 24.3, 26.4, 26.7, 28.3, 29.8, 31.17, 31.22, 31.33, 35.1, 35.48, 35.52, 35.8, 38.0, 39.9, 40.3, 42.9, 51.7, 56.2, 56.7, 63.1, 72.6, 174.9. IR (ν_{max} in cm^{-1}): 3508, 2935, 2866, 2100, 1715. HRMS *m*/*z*: calcd for $C_{26}H_{47}N_4O_3$ [M + NH_4]$^+$ 463.3643, found 463.3641.

*Methyl (4R)-4-((3S,5R,8R,9S,10S,13R,14S)-3-((4-(9-(2-((tert-Butoxycarbonyl)amino)ethyl)-7-ethynyl-9H-carbazol-2-yl)-1H-1,2,3-triazol-1-yl)methyl)-3-hydroxy-10,13-dimethylhexadecahydro-1H-cyclopenta[a]phenanthren-17-yl)pentanoate (**10**).* Compound **5** (21 mg, 0.06 mmol) and compound **9** (66 mg, 0.15 mmol, 2.5 equiv) were separately dissolved in 4 mL of DMF each and added to the reaction flask, followed by 20 mL of *t*BuOH. $CuSO_4$·$5H_2O$ (30 mg, 0.12 mmol, 2 equiv) and Na-L-ascorbate (47 mg, 0.24 mmol, 4 equiv) were separately dissolved in 2 mL of H_2O each and injected into the flask. The mixture was flushed for 15 min with N_2, heated to 60 °C, and stirred at that temperature for 24 h. The solvent was removed in vacuo. The crude was purified via flash chromatography (eluent 70:30 DCM/EtOAc), which yielded compound **10** as a brown powder (19 mg, 41%). ^{1}H NMR (400 MHz, $CDCl_3$) δ: 0.65 (s, 3H), 0.75−2.01 (m, 45H), 2.29 (m, 2H), 3.15 (s, 1H), 3.57 (s, 2H), 3.67 (s, 3H), 4.41 (s, 4H), 4.72 (dd, ^3J = 53.8 and 6.9 Hz, 2H), 4.86 (m, 1H), 7.34 (m, 1H), 7.51 (m, 2H), 7.93 (m, 2H), 8.08 (s, 1H), 8.29 (m, 1H). ^{13}C{^{1}H} NMR (101 MHz, $CDCl_3$) δ: 12.3, 18.5, 21.3, 23.8, 24.4, 26.5, 26.6, 28.4, 28.5, 29.9, 31.2, 31.3, 35.1, 35.6, 35.8, 38.0, 40.0, 40.3, 42.9, 51.7, 56.2, 56.6, 70.3, 72.0, 72.5, 74.4, 80.0, 112.9, 117.7, 119.8, 120.5, 121.2, 123.0, 123.2, 123.7, 141.2, 156.2, 166.3, 168.5, 175.1. HRMS *m*/*z*: calcd for $C_{49}H_{66}N_5O_5$ [M + H]$^+$ 804.5059, found 804.5062.

*Methyl (4R)-4-((3S,8S,9R,13S,14R)-3-((4-(9-(2-((tert-Butoxycarbonyl)amino)ethyl)-7-(1-(((3S,5R,8R,9S,10S,13R,14S)-3-hydroxy-17-((R)-5-methoxy-5-oxopentan-2-yl)-10,13-dimethylhexadecahydro-1H-cyclopenta[a]phenanthren-3-yl)methyl)-1H-1,2,3-triazol-4-yl)-9H-carbazol-2-yl)-1H-1,2,3-triazol-1-yl)methyl)-3-hydroxy-10,13-dimethylhexadeca-hydro-1H-cyclopenta[a]-phenanthren-17-yl)pentanoate (**11**).* Compound **10** (16 mg, 0.02 mmol) and compound **9** (72 mg, 0.16 mmol, 8 equiv) were separately dissolved in 4 mL of DMF each and added to the reaction flask, followed by 4 mL of *t*BuOH. $CuSO_4$·$5H_2O$ (10 mg, 0.04 mmol, 2 equiv) and Na-L-ascorbate (16 mg, 0.08 mmol, 4 equiv) were separately dissolved in 1 mL of H_2O each and added to the flask. The mixture was flushed for 15 min with N_2 and stirred at 60 °C for 24 h. The solvent was removed in vacuo, and the crude was purified via flash chromatography (eluent 70:30 EtOAc/hexane), yielding title compound **11** as a yellow powder (16 mg, 66%). ^{1}H NMR (700 MHz, $CDCl_3$) δ: 0.66 (s, 6H), 0.79−2.05 (m, 74H), 2.30 (m, 4H), 3.43 (m, 2H), 3.67 (s, 6H), 4.39 (m, 2H), 4.96 (s, 1H), 7.38−8.24 (m, 8H). ^{13}C{^{1}H} NMR (176 MHz, $CDCl_3$) δ: 12.2, 18.4, 21.3, 23.8, 24.4, 26.6, 26.7, 28.4, 28.5, 29.9, 30.0, 31.2, 31.3, 35.1, 35.6, 35.8, 38.0, 40.0, 40.3, 42.9, 51.6, 56.2, 56.7, 71.9, 117.6, 120.8, 123.0, 141.5, 175.0. HRMS *m*/*z*: calcd for $C_{75}H_{109}N_8O_8$ [M + H]$^+$ 1249.8363, found 1249.8373.

*2-(2-(1-(((3S,5R,8R,9S,10S,13R,14S)-3-Hydroxy-17-((R)-5-methoxy-5-oxopentan-2-yl)-10,13-dimethylhexadecahydro-1H-cyclopenta[a]phenanthren-3-yl)methyl)-1H-1,2,3-triazol-4-yl)-7-(1-(((3S,8S,9R,13S,14R)-3-hydroxy-17-((R)-5-methoxy-5-oxopentan-2-yl)-10,13-dimethylhexadecahydro-1H-cyclopenta[a]phenanthren-3-yl)methyl)-1H-1,2,3-triazol-4-yl)-9H-carbazol-9-yl)ethan-1-amonium Chloride (**R4**).* HCl (2 mL, 4 M) in dioxane was added to compound **11** (6.6 mg) and the mixture was stirred at rt for 1 h. Evaporation of the solvent in vacuo yielded receptor **R4** as a yellow powder quantitatively. ^{1}H NMR (400 MHz, DMF-d_7) δ: 0.66 (s, 6H), 0.82−2.11 (m, 85H), 2.30 (m, 4H), 3.64 (m, 8H), 4.51 (s, 4H), 5.08 (t, ^3J = 5.9 Hz, 2H), 7.93 (d, ^3J = 8.3 Hz, 2H), 8.26 (d, ^3J = 8.7 Hz, 2H), 8.53 (s, 2H), 8.84 (s, 2H), 9.02 (s, 3H). ^{13}C{^{1}H} NMR (101 MHz, DMF-d_7) δ: 12.7, 18.9, 22.0, 24.2, 25.0, 27.2, 27.7, 28.9, 31.5, 31.9, 32.2, 36.2, 36.7, 38.7, 39.9, 40.5, 41.1, 41.6, 43.6, 44.6, 51.9, 57.0, 57.4, 61.9, 62.4, 71.7, 72.1, 73.7, 107.3, 118.2, 121.7, 123.6, 124.2, 130.6, 142.7, 148.3, 175.0. ESI-MS *m*/*z*: calcd for $C_{70}H_{101}N_8O_6$ [M + H]$^+$ 1149.78386, found 1149.6.

*Methyl (4R)-4-((3R,8S,9R,13S,14R)-3-(2-(4-(9-(2-((tert-Butoxycarbonyl)amino)ethyl)-7-(1-(((3S,5R,8R,9S,10S,13R,14S)-3-hydroxy-17-((R)-5-methoxy-5-oxopentan-2-yl)-10,13-dimethylhexadecahydro-1H-cyclopenta[a]phenanthren-3-yl)methyl)-1H-1,2,3-triazol-4-yl)-9H-carbazol-2-yl)-1H-1,2,3-triazol-1-yl)acetoxy)-10,13-dimethylhexadecahydro-1H-cyclopenta[a]phenanthren-17-yl)-pentanoate (**12**).* Compound **10** (26 mg, 0.032 mmol) and compound **3** (30 mg, 0.064 mmol, 2 equiv) were dissolved in 2 mL of DMF, followed by the addition of 10 mL of *t*BuOH. $CuSO_4$·$5H_2O$ (16 mg, 0.064 mmol, 2 equiv) and Na-L-ascorbate (25 mg, 0.13 mmol, 4 equiv) were separately dissolved in 1 mL of H_2O each and added to the mixture. After 15 min flushing with N_2, the mixture was stirred at 60 °C for 24 h. The solvent was partially evaporated in vacuo, and the crude was purified via flash chromatography (eluent 70:30 DCM/EtOAc, followed by 60:40 DCM/EtOAc), yielding title compound **12** as a yellow powder (21 mg, 52%). ^{1}H NMR (700 MHz, $CDCl_3$) δ: 0.65 (m, 6H), 0.78−2.04 (m, 76H), 2.29 (m, 4H), 3.62 (m, 8H), 4.42 (m, 4H), 4.88 (m, 1H), 5.26 (m, 3H), 7.40−8.72 (m, 8H). ^{13}C{^{1}H} NMR (176 MHz, $CDCl_3$) δ: 12.3, 15.6, 18.5, 21.1, 21.3, 23.6, 23.8, 24.4, 26.5, 26.6, 26.8, 27.2, 28.4, 29.9, 31.2, 31.3, 31.4, 32.3, 34.8, 35.1, 35.6, 35.8, 35.91, 35.97, 40.0, 40.3, 40.7, 42.1, 42.9, 43.0, 51.7, 56.2, 56.6, 175.2. HRMS *m*/*z*: calcd for $C_{76}H_{109}N_8O_9$ [M + H]$^+$ 1277.8312, found 1277.8317.

*2-(2-(1-(((3S,5R,8R,9S,10S,13R,14S)-3-Hydroxy-17-((R)-5-methoxy-5-oxopentan-2-yl)-10,13-dimethylhexadecahydro-1H-cyclopenta[a]phenanthren-3-yl)methyl)-1H-1,2,3-triazol-4-yl)-7-(1-(2-(((3R,8S,9R,13S,14R)-17-((R)-5-methoxy-5-oxopentan-2-yl)-10,13-dimethylhexadecahydro-1H-cyclopenta[a]phenanthren-3-yl)oxy)-2-oxoethyl)-1H-1,2,3-triazol-4-yl)-9H-carbazol-9-yl)ethan-1-amonium Chloride (**R3**).* HCl (2 mL, 4 M) in dioxane was added to compound **12** (2.3 mg, 0.0018 mmol) at 0 °C, followed by stirring for 30 min at 0 °C. The solvent was removed with compressed air while keeping the solution at 0 °C. Title compound **R3** was obtained quantitatively as a yellow powder (2.2 mg). ^{1}H NMR (400 MHz, DMF-d_7) δ: 0.66 (s, 3H), 0.68 (s, 3H), 0.83−2.44 (m, 99H), 3.60 (m), 4.51 (s, 2H), 4.83 (m, 1H), 5.08 (t, ^3J = 6.5 Hz, 2H), 5.60 (s, 2H), 7.92 (double t, ^3J = 8.1 Hz, 2H), 8.28 (d, ^3J = 8.1 Hz, 2H), 8.52 (s, 2H), 8.81 (s, 1H), 8.93 (s, 1H), 8.95 (s, 3H). ^{13}C{^{1}H} NMR (101

DOI: 10.1021/acs.joc.9b01665
J. Org. Chem. XXXX, XXX, XXX−XXX

MHz, DMF-d_7) δ: 12.7, 19.0, 19.2, 21.8, 22.0, 23.5, 23.8, 24.2, 25.0, 27.3, 27.5, 27.9, 29.0, 31.6, 32.0, 33.1, 36.6, 36.9, 38.8, 40.5, 41.1, 41.3, 41.6, 42.8, 43.6, 46.8, 52.0, 57.0, 57.3, 62.0, 62.4, 64.5, 69.0, 69.6, 71.7, 72.0, 74.1, 77.1, 118.2, 121.7, 123.7, 130.7, 142.6, 148.2, 168.1, 175.0. HRMS m/z: calcd for $C_{71}H_{101}N_8O_7$ $[M + H]^+$ 1177.7788, found 1177.7775.

*2-Bromo-N-(((1R,4aS,10aR)-7-isopropyl-1,4a-dimethyl-1,2,3,4,4a,9,10,10a-octahydrophenanthren-1-yl)methyl)acetamide (**14**).* Dehydroabietylamine **13** (4.4 g, 9.2 mmol) was dissolved in 20 mL of dry DCM, followed by 3 mL of dry pyridine (36.8 mmol, 4 equiv). The mixture was cooled at 0 °C and bromoacetyl bromide (1.6 mL, 18.4 mmol, 2 equiv) was slowly added, followed by stirring at 0 °C for 1 h. The mixture was poured in a solution of 50 mL of H_2O and 30 mL of DCM. Due to poor phase separation, the mixture was centrifuged to isolate the bottom organic layer. $MgSO_4$ was added, the mixture was filtered, and the filtrate was evaporated in vacuo. Purification of the crude with flash chromatography (eluent 50:49:1 DCM/hexane/EtOAc) yielded compound **14** as a white powder (1.35 g, 36%). On NMR, a small impurity was observed (at 4.07 and 6.62 ppm), which could not be removed during purification. However, when performing the next reaction, removal of this impurity could be achieved (see compound **15**). ^{1}H NMR (400 MHz, $CDCl_3$) δ: 0.70−1.98 (m, 46H), 2.30 (d, ^3J = 12.9 Hz, 2H), 2.75−3.33 (m, 7H), 3.91 (m, 2H), 4.07 (m), 6.53 (m, 1H), 6.62 (m), 6.89 (s, 1H), 7.00 (d, ^3J = 8.2 Hz, 1H), 7.17 (d, ^3J = 8.2 Hz, 1H). ^{13}C{^{1}H} NMR (101 MHz, $CDCl_3$) δ: 18.75, 18.77, 19.3, 24.3, 25.6, 29.9, 30.6, 33.7, 36.5, 37.7, 38.5, 43.2, 45.9, 47.8, 50.4, 50.8, 51.1, 124.1, 124.5, 127.2, 134.9, 145.9, 147.1, 165.4. HRMS m/z: calcd for $C_{22}H_{36}BrN_2O$ $[M + NH_4]^+$ 423.2006, found 423.2022. Note: a peak corresponding to $[M + NH_4]^+$ + 4 Da was also observed, which is due to a reduced impurity that was present in the starting material (dehydroabietylamine). Because of the high similarity between both compounds, separation could not be achieved.

*2-Azido-N-(((1R,4aS,10aR)-7-isopropyl-1,4a-dimethyl-1,2,3,4,4a,9,10,10a-octahydrophenanthren-1-yl)methyl)acetamide (**15**).* Compound **14** (408 mg, 1 mmol) was dissolved in 15 mL of dry DMF, followed by the addition of 10 equiv NaN_3 (650 mg, 10 mmol) and stirring at rt for 24 h. The mixture was poured into 80 mL of H_2O and extracted with EtOAc. The organic phase was evaporated, and the crude was dry-loaded onto 2 g of silica. Purification via flash chromatography (eluent 70:30 hexane/EtOAc) yielded azide **15** as a transparent gel (304 mg, 82%). ^{1}H NMR (400 MHz, $CDCl_3$) δ: 0.69−1.98 (m, 50H), 2.30 (d, ^3J = 12.9 Hz, 2H), 2.75−3.34 (m, 7H), 4.00 (s, 2H), 6.31 (m, 1H), 6.90 (s, 1H), 7.00 (d, ^3J = 8.3 Hz, 1H), 7.17 (d, ^3J = 8.2 Hz, 1H). ^{13}C{^{1}H} NMR (101 MHz, $CDCl_3$) δ: 18.7, 18.9, 19.2, 24.2, 25.6, 30.5, 33.6, 36.4, 37.6, 37.7, 38.4, 45.6, 50.0, 52.9, 53.0, 124.1, 124.4, 127.2, 135.0, 146.0, 147.2, 166.7. IR (ν_{max} in cm^{-1}): 3316, 2925, 2867, 2101, 1655. HRMS m/z: calcd for $C_{22}H_{33}N_4O$ $[M + H]^+$ 369.2649, found 369.2661.

*tert-Butyl (2-(2,7-Bis(1-(2-((((1R,4aS,10aR)-7-isopropyl-1,4a-dimethyl-1,2,3,4,4a,9,10,10a-octahydrophenanthren-1-yl)methyl)amino)-2-oxoethyl)-1H-1,2,3-triazol-4-yl)-9H-carbazol-9-yl)ethyl)carbamate (**16**).* Compound **5** (20 mg, 0.057 mmol) was dissolved in 2 mL of DMF, followed by addition of 52 mg of compound **15** (0.14 mmol, 2.5 equiv) and 8 mL of *t*BuOH. $CuSO_4{\cdot}5H_2O$ (28 mg, 0.11 mmol, 2 equiv) and Na-L-ascorbate (45 mg, 0.23 mmol, 4 equiv) were separately dissolved in 1 mL of H_2O each and added to the mixture, followed by flushing for 15 min under N_2. The mixture was stirred at 60 °C for 24 h. The solvent was partially removed in vacuo and poured in 60 mL of H_2O, followed by extraction with DCM. The organic phase was evaporated, and the crude was purified via flash chromatography (eluent 60:40 EtOAc/DCM), yielding title compound **16** as a yellow powder (52 mg, 84%). ^{1}H NMR (400 MHz, $CDCl_3$) δ: 0.55−2.30 (m, 120H), 2.73−3.34 (m, 17H), 4.28 (s, 2H), 4.70 (s, 1H), 5.19 (s, 6H), 6.87 (s, 2H), 6.98 (d, ^3J = 8.6 Hz, 2H), 7.13 (d, ^3J = 8.6 Hz, 2H), 7.46 (m, 2H), 8.00 (m, 6H). ^{13}C{^{1}H} NMR (101 MHz, $CDCl_3$) δ: 18.65, 18.72, 19.3, 24.2, 25.5, 28.6, 28.8, 29.9, 30.4, 33.6, 36.4, 37.6, 37.8, 38.4, 46.0, 50.7, 53.8, 106.3, 117.3, 121.2, 123.1, 124.1, 124.4, 127.1, 134.9, 141.4, 145.9, 147.4, 165.4. ESI-MS m/z: calcd for $C_{69}H_{89}N_{10}O_5$ $[M + HOAc-OH]^-$ 1137.70174, found 1137.7.

*2-(2,7-Bis(1-(2-((((1R,4aS,10aR)-7-isopropyl-1,4a-dimethyl-1,2,3,4,4a,9,10,10a-octahydrophenanthren-1-yl)methyl)amino)-2-oxoethyl)-1H-1,2,3-triazol-4-yl)-9H-carbazol-9-yl)ethan-1-amonium Chloride (**R5**).* HCl (2 mL, 4 M) in dioxane was added to compound **16** (6.1 mg, 0.0056 mmol) and the mixture was stirred at rt for 1 h. Evaporation of the solvent with compressed air yielded receptor **R5** as a yellow powder quantitatively. ^{1}H NMR (400 MHz, DMF-d_7) δ: 0.71−2.39 (m, 137H), 3.03 (q, ^3J = 5.9 Hz, 2H), 3.22 (m, 4H), 4.14 (s, 1H), 4.21 (s, 1H), 4.29 (m, 2H), 4.61 (t, ^3J = 7.7 Hz, 4H), 5.40 (s, 4H), 6.91 (s, 2H), 7.02 (d, ^3J = 8.3 Hz, 2H), 7.22 (d, ^3J = 8.3 Hz, 2H), 7.84 (m, 2H), 8.23 (s, 2H), 8.27 (d, ^3J = 8.2 Hz, 2H), 8.44 (t, ^3J = 5.9 Hz, 2H), 8.51 (s, 3H), 8.79 (s, 2H). ^{13}C{^{1}H} NMR (101 MHz, DMF-d_7) δ: 19.5, 19.58, 19.79, 24.60, 24.63, 24.67, 26.0, 28.0, 29.3, 34.3, 36.9, 38.4, 38.6, 39.3, 40.3, 44.5, 44.6, 46.0, 50.7, 53.2, 62.0, 64.5, 69.0, 69.5, 72.0, 73.7, 74.2, 107.0, 118.0, 121.7, 123.3, 124.7, 125.3, 127.8, 130.2, 130.8, 136.0, 142.5, 146.4, 148.4, 148.7, 167.2. ESI-MS m/z: calcd for $C_{64}H_{81}N_{10}O_3$ $[M + HOAc-OH]^-$ 1037.64931, found 1037.6.

*3α-Bromoacetoxy-5β-cholan-24-oic Acid (**17**).* Lithocholic acid **1** (2 g, 5.3 mmol) was dissolved in 10 mL of dry THF. Pyridine (1.7 mL, 21.3 mmol, 4 equiv) was added and the mixture was cooled at 0 °C, followed by addition of 0.9 mL of bromoacetyl bromide (10.6 mmol, 2 equiv). The mixture was stirred at that temperature for 2 h. The reaction was quenched by addition of 20 mL of H_2O and extracted with DCM. The organic phase was evaporated in vacuo, and the residue was dissolved in DCM/MeOH (95:5) and dry-loaded onto 3 g of silica. Purification via flash chromatography (eluent 95:5 DCM/EtOAc) yielded compound **17** as a white solid (1.6 g, 60%). ^{1}H NMR (500 MHz, $CDCl_3$) δ: 0.65 (s, 3H), 0.83−2.01 (m, 36H), 2.33 (m, 2H), 3.80 (s, 2H), 4.79 (m, 1H). ^{13}C{^{1}H} NMR (126 MHz, $CDCl_3$) δ: 12.1, 18.3, 20.9, 23.3, 24.2, 26.3, 26.39, 26.42, 27.0, 28.2, 30.78, 30.83, 31.9, 34.6, 34.9, 35.3, 35.8, 40.1, 40.5, 41.9, 42.8, 56.0, 56.5, 76.7, 166.8, 179.3. HRMS m/z: calcd for $C_{26}H_{45}BrNO_4$ $[M + NH_4]^+$ 514.2527, found 514.2535.

*3α-Azidoacetoxy-5β-cholan-24-oic Acid (**18**).* Compound **17** (1 g, 2.0 mmol) was dissolved in 15 mL of dry DMF. NaN_3 (796 mg, 12 mmol, 6 equiv) was added and the mixture was stirred at rt for 24 h. Water (60 mL) was added, followed by extraction with EtOAc. The organic phase was evaporated in vacuo and the crude was purified via flash chromatography (first 99:1 DCM/EtOAc, then 95:5 DCM/EtOAc once the product started to elute). Compound **18** was obtained as a white powder (603 mg, 64%). ^{1}H NMR (400 MHz, $CDCl_3$) δ: 0.65 (s, 3H), 0.92 (m, 6H), 0.98−2.01 (m, 28H), 2.33 (m, 2H), 3.84 (s, 2H), 4.84 (m, 1H). ^{13}C{^{1}H} NMR (101 MHz, $CDCl_3$) δ: 12.2, 18.4, 21.0, 23.5, 24.4, 26.5, 26.8, 27.2, 28.4, 30.9, 31.1, 32.3, 34.8, 35.1, 35.5, 36.0, 40.3, 40.6, 42.1, 42.9, 50.8, 56.2, 56.6, 76.6, 168.0, 180.1. IR (ν_{max} in cm^{-1}): 3448, 2931, 2866, 2102, 1732, 1714, 1673, 1641. HRMS m/z: calcd for $C_{26}H_{45}N_4O_4$ $[M + NH_4]^+$ 477.3435, found 477.3443.

*(4R)-4-((3R,8S,9R,13S,14R)-3-(2-(4-(9-(2-((tert-Butoxycarbonyl)amino)ethyl)-7-(1-(2-(((3R,5R,8R,9S,10S,13R,14S)-17-((R)-4-carboxybutan-2-yl)-10,13-dimethylhexadecahydro-1H-cyclopenta[a]phenanthren-3-yl)oxy)-2-oxoethyl)-1H-1,2,3-triazol-4-yl)-9H-carbazol-2-yl)-1H-1,2,3-triazol-1-yl)acetoxy)-10,13-dimethylhexadecahydro-1H-cyclopenta[a]phenanthren-17-yl)pentanoic Acid (**R6**).* Compound **18** (603 mg, 1.3 mmol, 2.5 equiv) and compound **5** (188 mg, 0.52 mmol) were dissolved in 6 and 2 mL of DMF, respectively, and added to the reaction flask, followed by the addition of 20 mL of *t*BuOH. $CuSO_4{\cdot}5H_2O$ (262 mg, 1 mmol, 2 equiv) and Na-L-ascorbate (415 mg, 2.1 mmol, 4 equiv) were each dissolved in 2 mL of H_2O and added separately to the reaction. After flushing for 15 min under N_2, the mixture was stirred at 60 °C for 20 h. The solvent was removed in vacuo, and the crude was purified via flash chromatography (first 1:1 hexane/EtOAc + 1% HOAc, then 70:30 EtOAc/hexane + 1% HOAc). The collected fractions were dissolved in 40 mL of DCM and washed with H_2O to remove the HOAc. Evaporation of the organic phase yielded receptor **R6** as a white powder (372 mg, 56%). ^{1}H NMR (300 MHz, $CDCl_3$) δ: 0.64 (s, 7H), 0.78−2.19 (m, 112H), 2.31 (m, 4H), 3.64 (m, 2H), 4.53 (m, 2H), 4.87 (m, 2H), 4.97 (m,

DOI: 10.1021/acs.joc.9b01665
J. Org. Chem. XXXX, XXX, XXX−XXX

1H), 5.23 (s, 4H), 7.65 (d, ^3J = 8.6 Hz, 2H), 8.07 (m, 6H). $^{13}C\{^1H\}$ NMR (75 MHz, $CDCl_3$) δ: 12.2, 18.4, 21.0, 23.5, 24.3, 26.4, 26.7, 27.2, 28.4, 28.5, 29.9, 31.0, 32.2, 34.7, 35.1, 35.6, 35.9, 39.8, 40.3, 40.6, 42.1, 42.9, 51.7, 56.0, 56.6, 106.4, 117.8, 121.0, 121.7, 123.1, 128.1, 141.7, 149.0, 165.9, 179.2. HRMS m/z: calcd for $C_{75}H_{105}N_8O_{10}$ $[M + H]^+$ 1277.7948, found 1277.7968.

Immobilization of R6 on Solid Support. Dry DMF (2 mL) was added to 29 mg of 3-aminopropyl-functionalized silica (loading 1 mmol/g), followed by addition of receptor **R6** (33 mg, 0.026 mmol, 1 equiv), HBTU (59 mg, 0.16 mmol, 6 equiv), and DIPEA (0.03 mL, 0.16 mmol, 6 equiv). The mixture was shaken at rt for 24 h. The solvent was filtered off, and the residue was rinsed with DMF and DCM, yielding 33 mg of immobilized **R6** (51% yield). As expected, TNBS test showed red coloration, thus indicating the presence of free amines. Therefore, a capping step was performed as follows: 2 mL of dry DMF was added to the resin, followed by addition of 0.05 mL of Ac_2O (0.58 mmol, 20 equiv) and 0.08 mL of Et_3N (0.58 mmol, 20 equiv). The mixture was shaken for 24 h at rt. The solvent was filtered off, and the resin was washed with DMF and DCM. Full capping was confirmed with the TNBS test. Finally, 2 mL of 4 M HCl in dioxane was added to the resin and the mixture was shaken for 1 h at rt. The solvent was filtered off, and the residue was washed with DCM. TNBS test showed intense red coloration of the beads, thus indicating successful Boc deprotection.

Acetylation of the Solid Support. Dry DMF (2 mL) was added to 146 mg of 3-aminopropyl-functionalized silica (loading 1 mmol/g), followed by 0.14 mL of Ac_2O (1.46 mmol, 10 equiv) and 0.2 mL of Et_3N (1.46 mmol, 10 equiv). The mixture was shaken at rt for 24 h. The solvent was filtered off, and the residue was washed with DMF and DCM, yielding 127 mg of acetylated resin (83%). The TNBS test was colorless, thus indicating complete acetylation.

SPE Experiments. The resins (3-aminopropyl-functionalized silica (Si-NH_2), Si-NHAc, and Si-R6) were placed in reaction vessels for peptide synthesis containing a microporous filter. Beauvericin or valinomycin solution (3 mL, 100 nM) in hexane was added, and the mixture was shaken overnight (the BEA and VAL solutions were prepared from 2.8 and 1 mM stock solutions in $CHCl_3$, respectively). The next day, the solvent was filtered off and kept aside (=rest fraction). The resin was eluted with 3 mL of the appropriate solvent, as shown in Figure 8. The collected fractions were evaporated, and the residue in each sample was reconstituted in 1 mL of MeOH. Quantification of the BEA or VAL concentration in each sample was performed via LC–MS/MS, as reported previously,[35] by determining the area under the curve in the total ion count chromatogram of the most abundant product ion (244.3 Da for BEA and 343.5 Da for VAL).

Fluorescence Titrations. Fluorescence measurements were performed on a Cary Eclipse Fluorescence Spectrophotometer (Varian Australia Pty. Ltd.). The slit width for both excitation and emission was 5 nm. The temperature was maintained at 25 °C during the measurements. For receptor **R2**, the following parameters were used: photomultiplier tube (PMT) voltage = 420 V, λ_{ex} = 329 nm, λ_{em} = 340–800 nm. A 10 μM solution of receptor **R2** was prepared by adding 62.4 μL of a 0.4 mM stock solution in $CHCl_3$ to a cuvette containing 2438 μL of $CHCl_3$. After recording the emission spectrum, beauvericin was added (from a 1 mM stock solution) in amounts corresponding to 0.1, 0.2, 0.3, 0.5, 0.7, 1, 1.5, 2, 3, 4, and 5 equiv (in total), and the fluorescence intensity was measured in between each addition.

The titrations of the receptor analogues with the different ionophores were done similar to what has been described for **R2** and BEA. All receptors were excited at λ_{ex} = 329 nm in $CHCl_3$, and titrations were performed in triplicate. Depending on the receptor, different concentrations and PMT voltages were used. Fitting of the titration data was done similar to what has been described for **R2**, except the used maximum λ_{em} was dependent on the receptor (Table S1).

Cell Experiments: Cell Growth. HepG2 cells were grown in T25 or T75 flasks containing 4 or 12 mL of growth medium, respectively. The growth medium contained 10% fetal bovine serum, 1% antibiotics (PenStrep, 10 000 units/mL penicillin + 10 000 μg/mL streptomycin, purchased from Gibco, Thermo Fisher), and 1% nonessential amino acids and cell medium (Dulbecco's modified Eagle's medium + GlutaMAX, purchased from Gibco, Thermo Fisher). Cells were incubated in an atmosphere containing 5% CO_2.

Preparation of the Well Plates. Once the cells had a suitable confluence, they were trypsinized and reconstituted in growth medium. Of this cell suspension, 100 μL was taken and added to an eppendorf tube containing 100 μL of trypan blue staining solution (0.4%). A fraction of this mixture was added to a Bürker counting chamber, and the number of cells were counted manually using a light microscope. Once the cell concentration was known, cell solutions were prepared in such a way that each well contained 0.2 mL of medium and 40 000 cells. The outer wells were filled with phosphate-buffered saline (PBS) only and did not contain any cells. The resulting plates are then incubated overnight. The next day, the treatment was performed (vide infra).

General Procedure for Performing the MTT Assay. After the treatment, 100 μL of medium was removed from each well and 20 μL of the MTT solution was added (5 mg/mL in PBS, 0.22 μm filter sterilized). The plate was incubated for 2 h at 37 °C. The liquid was completely removed from each well, and 200 μL DMSO was added. The solution was pipetted up and down to homogenize, and the UV–vis absorbance was measured at 570 nm using a plate reader.

General Procedure for Performing the SRB Assay. After the treatment, 50 μL of a trichloroacetic acid solution (50% in Milli-Q water) was added, followed by storage of the plate at 4 °C for 1 h. The plate was carefully rinsed with tap water multiple times. Once dry, 200 μL SRB staining solution was added (0.4% in 1% acetic acid). After 30 min, the plate was rinsed with 1% acetic acid to remove the unbound dye (three times), followed by drying. Then, 200 μL of a 10 mM Tris buffer solution was added and each well was properly homogenized. The UV–vis absorbance was measured at 490 nm using a plate reader.

General Procedure for Performing the NR Assay. After the treatment, each well was washed once with growth medium (without antibiotics or serum). The NR staining solution was made by adding 0.3 mL of a NR stock solution to 30 mL of growth medium (without antibiotics or serum). The stock solution was prepared by dissolving 40 mg of neutral red dye in 10 mL of PBS. The solution was first placed in a water bath at 37 °C for 30 min to assure solubility of the dye, followed by filtration through a 0.22 μm filter. Then, the liquid in each well was replaced by 100 μL of this staining solution and the plates were incubated at 37 °C for 3 h. The cells were washed once with PBS and dried. Then, 100 μL of desorption solution was added (1% HOAc, 50% EtOH, and 49% H_2O). After 20 min, the UV–vis absorbance is measured at 540 nm using a plate reader.

Treatment of the Cells. The growth medium was removed from the plate (which was prepared as described in Preparation of the Well Plates). The wells were subsequently filled with 200 μL of the appropriate treatment condition (see preparation below).

Treatment with BEA Alone. Taking the 5 μM BEA treatment condition as an example, a diluted solution **A** was made by taking 20 μL of the BEA stock solution (6.378×10^{-3} M, in DMF), followed by addition of 180 μL of DMF. Then, 47 μL of **A** was taken and added to a falcon tube together with 13 μL of DMF. Then, this was added to 5940 μL of growth medium. For the 2.5 μM BEA condition, 24 μL of **A** was taken and added to a falcon tube containing 36 μL of DMF. Then, this was added to 5940 μL of growth medium. For the 1% DMF condition, 60 μL of DMF was added to a falcon tube containing 5940 μL of growth medium. The other treatment conditions were prepared in an analogous way. Note that the total DMF volume was always kept constant, namely, 1%. The plate was incubated for 24 h at 37 °C and stained according to the general MTT staining procedure described above. The same procedure was followed for the plates stained with SRB or NR.

Treatment with R2 Alone. Taking the 100 μM solution as an example, 66 μL from a 1.82×10^{-5} M stock solution of **R2** (in DMF) was added to 174 μL of DMF (=solution **B**). From this solution, 60 μL was taken and added to 5940 μL of growth medium. For the 50

DOI: 10.1021/acs.joc.9b01665
J. Org. Chem. XXXX, XXX, XXX–XXX

μM solution, 120 μL of **B** was taken and added to 120 μL of DMF. From this solution, 60 μL was taken and added to 5940 μL of growth medium. The other treatment solutions were prepared in a similar fashion, while making sure that the total DMF percentage was always kept constant (1%). The plate was incubated for 24 h at 37 °C and stained according to the general MTT staining procedure described above. The same procedure was followed for the plates stained with SRB or NR.

Treatment with BEA + R2. Taking the 5 μM BEA + 10 equiv **R2** treatment condition as an example, 20 μL of a 6.38 × 10^{-3} M stock solution of BEA (in DMF) was added to 80 μL of DMF (=solution **C**). From a stock solution of **R2** (1.82 × 10^{-5} M in DMF), 50 μL is taken and added to 50 μL of DMF (=solution **D**). Then, 16.5 μL is taken from this solution and added to a mixture containing 23.5 μL of solution **C** and 20 μL of DMF. This solution was subsequently added to 5940 μL of growth medium. For the 5 μM BEA treatment solution, 23.5 μL of solution **C** was added to 36.5 μL of DMF and the resulting mixture was added to 5940 μL of growth medium. While for the 10 equiv **R2** treatment solution, 16.5 μL of solution **D** was added to 43.5 μL DMF and the resulting mixture was added to 5940 μL of growth medium. The other treatment solutions were prepared in a similar fashion while making sure that the total DMF concentration always remained constant (1%). The plate was incubated for 24 h at 37 °C and stained according to the general MTT staining procedure described above. The same procedure was followed for the plates stained with SRB or NR.

Treatment with Boc-Protected Receptor 6. The treatment solutions were prepared in a similar fashion to BEA + **R2** using a 1.82 × 10^{-5} M stock solution of **6** (in DMF). The plate was incubated for 24 h at 37 °C and stained according to the general MTT staining procedure described above.

■ ASSOCIATED CONTENT

Supporting Information

The Supporting Information is available free of charge on the ACS Publications website at DOI: 10.1021/acs.joc.9b01665.

Spectroscopic characterization, used equations for the data fitting, additional fluorescence titration spectra, and results from cell assays (PDF)

■ AUTHOR INFORMATION

Corresponding Author

*E-mail: Annemieke.Madder@Ugent.be.

ORCID

Sarah De Saeger: 0000-0002-2160-7253

Annemieke Madder: 0000-0003-0179-7608

Notes

The authors declare the following competing financial interest(s): The technology described in the manuscript is part of a pending patent application by V.O., A.R., B.S., S.D.S. and A.M.

■ ACKNOWLEDGMENTS

The authors thank Charlotte Grootaert for her guidance in the practical aspects of the cell experiments. This research was funded by the BOF Special Research Fund from Ghent University, GOA project no. 01G02213. V.O. is grateful to the Fonds voor Wetenschappelijk Onderzoek for a VLAIO research grant.

■ REFERENCES

(1) Valderrama, W. B.; Dudley, E. G.; Doores, S.; Cutter, C. N. Commercially Available Rapid Methods for Detection of Selected Food-borne Pathogens. *Crit. Rev. Food Sci. Nutr.* **2016**, *56*, 1519−1531.

(2) Hardstaff, J. L.; Clough, H. E.; Lutje, V.; McIntyre, K. M.; Harris, J. P.; Garner, P.; O'Brien, S. J. Foodborne and Food- Handler Norovirus Outbreaks: A Systematic Review. *Foodborne Pathog. Dis.* **2018**, *15*, 589−597.

(3) Gupta, S.; Krasnoff, S. B.; Underwood, N. L.; Renwick, J. A. A.; Roberts, D. W. Isolation of Beauvericin as an Insect Toxin from *Fusarium semitectum* and *Fusarium moniliforme* var. Subglutinans. *Mycopathologia* **1991**, *115*, 185−189.

(4) Shemyakin, M. M.; Ovchinnikov, Y. A.; Kiryushkin, A. A.; Ivanov, V. T. The Structure and Total Synthesis of Enniatin B. *Tetrahedron Lett.* **1963**, *4*, 885−890.

(5) Uhlig, S.; Torp, M.; Heier, B. T. Beauvericin and Enniatins A, A1, B and B1 in Norwegian Grain: A Survey. *Food Chem.* **2006**, *94*, 193−201.

(6) Ritieni, A.; Moretti, A.; Logrieco, A.; Bottalico, A.; Randazzo, G.; Monti, S. M.; Ferracane, R.; Fogliano, V. Occurrence of Fusaproliferin, Fumonisin B1, and Beauvericin in Maize from Italy. *J. Agric. Food Chem.* **1997**, *45*, 4011−4016.

(7) Juan, C.; Mañes, J.; Raiola, A.; Ritieni, A. Evaluation of Beauvericin and Enniatins in Italian Cereal Products and Multicereal Food by Liquid Chromatography Coupled to Triple Quadrupole Mass Spectrometry. *Food Chem.* **2013**, *140*, 755−762.

(8) Kouri, K.; Lemmens, M.; Lemmens-Gruber, R. Beauvericin-Induced Channels in Ventricular Myocytes and Liposomes. *Biochim. Biophys. Acta, Biomembr.* **2003**, *1609*, 203−210.

(9) Tonshin, A. A.; Teplova, V. V.; Andersson, M. A.; Salkinoja-Salonen, M. S. The Fusarium Mycotoxins Enniatins and Beauvericin Cause Mitochondrial Dysfunction by Affecting the Mitochondrial Volume Regulation, Oxidative Phosphorylation and Ion Homeostasis. *Toxicology* **2010**, *276*, 49−57.

(10) Jow, G.-M.; Chou, C.-J.; Chen, B.-F.; Tsai, J.-H. Beauvericin Induces Cytotoxic Effects in Human Acute Lymphoblastic Leukemia Cells Through Cytochrome c Release, Caspase 3 Activation: The Causative Role of Calcium. *Cancer Lett.* **2004**, *216*, 165−173.

(11) Rodríguez-Carrasco, Y.; Heilos, D.; Richter, L.; Süssmuth, R. D.; Heffeter, P.; Sulyok, M.; Kenner, L.; Berger, W.; Dornetshuber-Fleiss, R. Mouse Tissue Distribution and Persistence of the Food-born Fusariotoxins Enniatin B and Beauvericin. *Toxicol. Lett.* **2016**, *247*, 35−44.

(12) Taevernier, L.; Bracke, N.; Veryser, L.; Wynendaele, E.; Gevaert, B.; Peremans, K.; De Spiegeleer, B. Blood-Brain Barrier Transport Kinetics of the Cyclic Depsipeptide Mycotoxins Beauvericin and Enniatins. *Toxicol. Lett.* **2016**, *258*, 175−184.

(13) Langton, M. J.; Serpell, C. J.; Beer, P. D. Anion Recognition in Water: Recent Advances from a Supramolecular and Macromolecular Perspective. *Angew. Chem., Int. Ed.* **2016**, *55*, 1974−1987.

(14) Gokel, G. W.; Leevy, W. M.; Weber, M. E. Crown Ethers: Sensors for Ions and Molecular Scaffolds for Materials and Biological Models. *Chem. Rev.* **2004**, *104*, 2723−2750.

(15) Mazik, M. Molecular Recognition of Carbohydrates by Acyclic Receptors Employing Noncovalent Interactions. *Chem. Soc. Rev.* **2009**, *38*, 935−956.

(16) Canevet, D.; Pérez, E. M.; Martín, N. Wraparound Hosts for Fullerenes: Tailored Macrocycles and Cages. *Angew. Chem., Int. Ed.* **2011**, *50*, 9248−9259.

(17) Shinoda, S.; Tsukube, H. Molecular Recognition of Cytochrome c by Designed Receptors for Generation of In Vivo and In Vitro Functions. *Chem. Sci.* **2011**, *2*, 2301−2305.

(18) Chinai, J. M.; Taylor, A. B.; Ryno, L. M.; Hargreaves, N. D.; Morris, C. A.; Hart, P. J.; Urbach, A. R. Molecular Recognition of Insulin by a Synthetic Receptor. *J. Am. Chem. Soc.* **2011**, *133*, 8810−8813.

(19) Schmuck, C.; Rupprecht, D.; Wienand, W. Sequence-Dependent Binding of Dipeptides by an Artificial Receptor in Water. *Chem. − Eur. J.* **2006**, *12*, 9186−9195.

(20) Bernard, J.; Wennemers, H. Macrocyclic Diketopiperazine Receptors: Effect of Macrocyclization on the Binding Properties of Two-Armed Receptors. *Org. Lett.* **2007**, *9*, 4283−4286.

DOI: 10.1021/acs.joc.9b01665
J. Org. Chem. XXXX, XXX, XXX−XXX

(21) Gersthagen, T.; Hofmann, J.; Klärner, F.-G.; Schmuck, C.; Schrader, T. Ditopic Arginine-Aspartate Binders Recognize RGD Loops. *Eur. J. Org. Chem.* **2013**, *2013*, 1080−1092.
(22) Ornelis, V.; Rajkovic, A.; Sas, B.; De Saeger, S.; Madder, A. Development of a Synthetic Receptor for the Food Toxin Beauvericin: A Tale of Carbazole and Steroids. *Org. Lett.* **2018**, *20*, 6368−6371.
(23) Sonogashira, K.; Tohda, Y.; Hagihara, N. A Convenient Synthesis of Acetylenes: Catalytic Substitutions of Acetylenic Hydrogen with Bromoalkenes, Iodoarenes and Bromopyridines. *Tetrahedron Lett.* **1975**, *16*, 4467−4470.
(24) Rostovtsev, V. V.; Green, L. G.; Fokin, V. V.; Sharpless, K. B. A Stepwise Huisgen Cycloaddition Process: Copper(I)-Catalyzed Regioselective "Ligation" of Azides and Terminal Alkynes. *Angew. Chem., Int. Ed.* **2002**, *41*, 2596−2599.
(25) Han, G.; Tamaki, M.; Hruby, V. J. Fast, Efficient and Selective Deprotection of the Tert-Butoxycarbonyl (Boc) Group Using HCl/dioxane (4M). *J. Pept. Res.* **2001**, *58*, 338−341.
(26) van de Weert, M. Fluorescence Quenching to Study Protein-ligand Binding: Common Errors. *J. Fluoresc.* **2010**, *20*, 625−629.
(27) Ulatowski, F.; Dabrowa, K.; Balakier, T.; Jurczak, J. Recognizing the Limited Applicability of Job Plots in Studying Host-Guest Interactions in Supramolecular Chemistry. *J. Org. Chem.* **2016**, *81*, 1746−1756.
(28) Hibbert, D. B.; Thordarson, P. The Death of the Job Plot, Transparency, Open Science and Online Tools, Uncertainty Estimation Methods and Other Developments in Supramolecular Chemistry Data Analysis. *Chem. Commun.* **2016**, *52*, 12792−12805.
(29) Aher, N. G.; Pore, V. S.; Mishra, N. N.; Shukla, P. K.; Gonnade, R. G. Design and Synthesis of Bile Acid-Based Amino Sterols as Antimicrobial Agents. *Bioorg. Med. Chem. Lett.* **2009**, *19*, 5411−5414.
(30) González, M. A. Synthetic Derivatives of Aromatic Abietane Diterpenoids and their Biological Activities. *Eur. J. Med. Chem.* **2014**, *87*, 834−842.
(31) Huang, W.-G.; Wang, H.-S.; Huang, G.-B.; Wu, Y.-M.; Pan, Y.-M. Enantioselective Friedel-Crafts Alkylation of N-Methylindoles with Nitroalkenes Catalyzed by Chiral Bifunctional Abietic-Acid-Derived Thiourea-Zn^{II} Complexes. *Eur. J. Org. Chem.* **2012**, *2012*, 5839−5843.
(32) Laaksonen, T.; Heikkinen, S.; Wähälä, K. Synthesis and Applications of Secondary Amine Derivatives of (+)-Dehydroabietylamine in Chiral Molecular Recognition. *Org. Biomol. Chem.* **2015**, *13*, 10548−10555.
(33) Fei, B.-L.; Yin, B.; Li, D.-D.; Xu, W.-S.; Lu, Y. Enantiopure Copper(II) Complex of Natural Product Rosin Derivative: DNA Binding, DNA Cleavage and Cytotoxicity. *J. Biol. Inorg. Chem.* **2016**, *21*, 987−996.
(34) Serrano, A. B.; Capriotti, A. L.; Cavaliere, C.; Piovesana, S.; Samperi, R.; Ventura, S.; Laganà, A. Development of a Rapid LC-MS/MS Method for the Determination of Emerging Fusarium Mycotoxins Enniatins and Beauvericin in Human Biological Fluids. *Toxins* **2015**, *7*, 3554−3571.
(35) Decleer, M.; Rajkovic, A.; Sas, B.; Madder, A.; De Saeger, S. Development and Validation of Ultra-High-Performance Liquid Chromatography-Tandem Mass Spectrometry Methods for the Simultaneous Determination of Beauvericin, Enniatins (A, A1, B, B1) and Cereulide in Maize, Wheat, Pasta and Rice. *J. Chromatogr. A* **2016**, *1472*, 35−43.
(36) Mallebrera, B.; Brandolini, V.; Font, G.; Ruiz, M. Cytoprotective Effect of Resveratrol Diastereomers in CHO-K1 Cells Exposed to Beauvericin. *Food Chem. Toxicol.* **2015**, *80*, 319−327.
(37) Pócsfalvi, G.; Di Landa, G.; Ferranti, P.; Ritieni, A.; Randazzo, G.; Malorni, A. Observation of Non-Covalent Interactions Between Beauvericin and Oligonucleotides Using Electrospray Ionization Mass Spectrometry. *Rapid Commun. Mass Spectrom.* **1997**, *11*, 265−272.
(38) Tomoda, H.; Huang, X.-H.; Cao, J.; Nishida, H.; Nagao, R.; Okuda, S.; Tanaka, H.; Omura, S.; Arai, H.; Inoue, K. Inhibition of Acyl-CoA: Cholesterol Acyltransferase Activity by Cyclodepsipeptide Antibiotics. *J. Antibiot.* **1992**, *45*, 1626−1632.
(39) Sieuwerts, A. M.; Klijn, J. G. M.; Peters, H. A.; Foekens, J. A. The MTT Tetrazolium Salt Assay Scrutinized: How to Use this Assay Reliably to Measure Metabolic Activity of Cell Cultures In Vitro for the Assessment of Growth Characteristics, IC50-Values and Cell Survival. *Eur. J. Clin. Chem. Clin. Biochem.* **1995**, *33*, 813−823.
(40) Repetto, G.; del Peso, A.; Zurita, J. L. Neutral Red Uptake Assay for the Estimation of Cell Viability/Cytotoxicity. *Nat. Protoc.* **2008**, *3*, 1125−1131.
(41) Vichai, V.; Kirtikara, K. Sulforhodamine B Colorimetric Assay for Cytotoxicity Screening. *Nat. Protoc.* **2006**, *1*, 1112−1116.
(42) Juan-García, A.; Ruiz, M.-J.; Font, G.; Manyes, L. Enniatin A1, Enniatin B1 and Beauvericin on HepG2: Evaluation of Toxic Effects. *Food Chem. Toxicol.* **2015**, *84*, 188−196.
(43) EFSA Panel on Contaminants in the Food Chain (CONTAM). Scientific Opinion on the Risks to Human and Animal Health Related to the Presence of Beauvericin and Enniatins in Food and Feed. *EFSA J.* **2014**, *12*, 3802.
(44) Umali, A. P.; Anslyn, E. V. A General Approach to Differential Sensing Using Synthetic Molecular Receptors. *Curr. Opin. Chem. Biol.* **2010**, *14*, 685−692.

DOI: 10.1021/acs.joc.9b01665
J. Org. Chem. XXXX, XXX, XXX−XXX